REVIEWS OF MODERN PHYSICS

The Linear Momenta of Electrons in Atoms and in Solid Bodies as Revealed by X-Ray Scattering

Jesse W. M. DuMond, *California Institute of Technology, Pasadena*

Table of Contents

A. Introduction

THE purpose of this paper is to describe a series of related experiments revealing a new physical effect predicted by the author in 1929.[1, 2] These predictions have been completely verified by the experimental results of the author in collaboration with H. A. Kirkpatrick. A very simple interpretation of these results would seem to lead us to direct evidence as to the dynamic nature of atoms.

Ever since the epoch-making theory of Niels

Bohr, physicists have thought of the atom as a dynamic entity. The great successes of the Bohr picture of an atom as a small solar system consisting of a nucleus round which electrons circulated in stable orbits, gave assurance that the picture must contain at least important elements of truth. The quantitative explanation of the frequencies of the spectral lines in the light emitted by hydrogen based on this picture is, of course, its most striking success. Mention should also be made of the phenomenon known as the "Mitbewegung des Kerns" which, by means of the Bohr picture, explains, with beautiful quantitative accuracy, the slight displacement of cer-

[1] Jesse W. M. DuMond, Phys. Rev. [2] 33, 643 (1929).
[2] Jesse W. M. DuMond, Phys. Rev. [2] 36, 146 (1930).

tain lines in the spectrum of ionized helium away from the position of certain of the hydrogen lines. Chemists were somewhat slower to adopt the idea of a dynamic atom, perhaps because the phenomena of interest to the chemist did not require it. Static atom models sufficient to explain many chemical properties of atoms have not even yet been entirely abandoned insofar as they furnish useful interpretations of chemical phenomena.

The orbits of Bohr described by point electrons have given place to the more modern quantum mechanical models. The electron is shown to have periodic properties so that the description of the dynamic atom model may be made in terms of waves ceaselessly beating about the nucleus. In this description, however, very much of the original picture of Bohr remains. The electron can no longer be sharply localized in space and time, but must be described by an undulatory complex imaginary function ψ, the square of whose amplitude expresses the *probability* that an observation will reveal the presence of the electron. Nevertheless, the Hamiltonian function for what is essentially the atom of Bohr with point electrons is still the controlling factor in determining the equation satisfied by these waves. As A. Sommerfeld has succinctly said, the atom of the new quantum mechanics is a *Verschwachenes Gebild* of the Bohr atom.

Just as the Bohr atom model endowed its electrons with motion, so the atom model of wave mechanics is possessed of internal momentum—it is a dynamic atom. Like the position of an electron its momentum is no longer a sharply defined quantity but one whose probability of observation under the definite conditions of some ideal experiment can be computed. It has been shown, however,[3] that the root mean square value of the total momentum averaged over its various probabilities is equal to the momentum of the corresponding Bohr electron. Kinematic terms such as "motion" and "velocity" are no longer strictly applicable to electrons in atoms since such terms refer to the time derivative of the electron's position which is not sharply defined. But dynamic terms such as impulse and linear momentum have validity when applied to the internal structure of the atom from the standpoint

[3] Boris Podolsky and Linus Pauling, Phys. Rev. [2] 34, 109 (1929).

of quantum mechanics. The experiments about to be described reveal the presence of the linear momenta of the electrons in the atom as well as the momenta of the so-called "free" electrons in metals whose presence accounts for metallic electrical conductivity. The atom behaves toward radiation used to examine it very much as though it contained electrons in ceaseless motion with the tremendous velocities predicted by Bohr. Its behavior is in still better accord, however, with the predictions of quantum mechanics.

We have become so accustomed to the ideas involved in quantum mechanics that we are prone to forget the experimental foundation which supports these ideas. Up to the time of the experiments here described, there existed not one shred of direct experimental evidence for internal linear momentum in atoms. The multitudinous observations of spectroscopy gave information as to the changes in *energy* that atoms might undergo. These changes in energy were explainable in terms of a theory of atoms assumed dynamic in nature. No evidence *contrary* to this assumption has appeared but the absence of contrary evidence is clearly a very weak argument. The experiments of the author and his coworkers here described give direct evidence of the presence of linear electron momenta in the atom and hence are of importance in rounding out the validity of modern atomic theory.

The investigation consists in observing the spectral modifications introduced by the process of scattering an initially monochromatic x-ray beam under a sharply defined scattering angle by a scattering body consisting of the atoms in which the linear electron momenta are to be studied. Under these conditions two types of scattering occur, called modified and unmodified scattering, respectively. In the case of the modified scattering there is an exchange of momentum between the electrons and the radiation so that not only does the radiation impart momentum to the electrons but the electrons also leave the imprint of their initial momenta on the radiation as it is observed in the scattered beam. This experiment differs from most other spectroscopic observations in that *momentum* is of importance rather than *energy*. In the unmodified type of scattering the exchange of momentum occurs between the radiation and the atom as a whole and,

as the mass of the atom is relatively very large, there is no observable modification of the scattered radiation.

In 1925, G. E. M. Jauncey[4] proposed a theory according to which the modified line discovered by Arthur Compton should possess a broader spectral structure than the corresponding line in the primary radiation. This theory assumed the interaction of the initial electron momentum with the radiation in the process of modified scattering. Unfortunately, Jauncey's theory introduced the characteristic momenta of electrons in classical Bohr stationary orbits *ab initio* with the result that the spectral structure of the modified line predicted by this theory contained the faults, as well as the virtues, of the Bohr atom model. Furthermore, the theory was not generalized so as to readily permit the introduction of *any* momentum distribution and the physical interpretation was somewhat masked by the analytical complexities. In particular, the unwary might be led to attach too much importance from this theory to the statement that the *position* of the electron in its orbit determines whether the electron will scatter radiation with or without modification. Jauncey's important and ingenious contribution was the idea that when the electron's initial momentum was properly related to the momenta of the incident and scattered radiation, the electron could acquire enough energy to overcome its binding energy and would then be free to escape with a certain part of the radiant energy, and thus modified scattering would result. The unmodified scattering was to be associated with those cases where the relation between initial electron momentum and the radiation momenta would not permit the electron to receive energy in excess of its binding energy in accord with the laws of conservation of momentum and energy. The change in momentum of the radiation on scattering was then absorbed by the atom as a whole rather than by the electron.

An analysis of the scattering of radiation by a free electron with initial momentum was made by L. de Broglie[5] in 1926. It is easy to show from this analysis that the change in wave-length of

the radiation will consist of two terms, one of which corresponds to the justly famous Compton shift, while the other is of the nature of a Doppler effect ascribable to the initial velocity of the free electron.

It is for this reason that a very simple interpretation of the spectral broadening of modified scattered x-radiation can be given. The phenomenon may be regarded as a *Doppler broadening* in almost complete analogy with the well-known Doppler broadening of spectral lines from the rapidly moving atoms in chaotic thermal agitation in a very hot source of light. The analogy fails in that the electrons in the case of modified x-ray scattering are not primary sources of radiation, but scattering agents. It therefore becomes important to consider carefully the Doppler effect of a moving scattering particle.

B. Theory

1. Doppler change of wave-length caused by the motion of a scattering particle

The Doppler effect is usually understood to mean a change in the frequency of radiation caused by relative motion of the source and the observer. Referring to Fig. 1, the wave-length
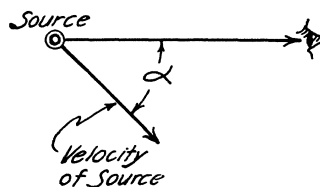
Fig. 1. Doppler effect of a moving source of radiation.

change due to a source velocity v at angle α with the direction of observation is given by the relation

$$\Delta\lambda/\lambda = (v/c) \cos \alpha. \tag{1}$$

This is an approximate formula applicable when $\Delta\lambda/\lambda \ll 1$. It is a well-known fact that this change in wave-length or frequency can be deduced from the application of the laws of conservation of energy and momentum to the moving emitting source if we associate an energy $h\nu$ and a momentum $h\nu/c$ with each photon emitted.[6] The term

[4] G. E. M. Jauncey, Phys. Rev. [2] 25, 314 (1925); 723 (1925).

[5] L. de Broglie, *Ondes et Mouvements*, Fasicule 1, 94 (1926).

[6] A. Sommerfeld, *Atombau und Spektrallinien*, pp. 53–55, fourth edition.

Doppler effect is commonly extended to include the case of wave-length change caused by reflection from a moving mirror. Here, though the source is fixed relative to the observer, the motion of the image of the source in the mirror reduces this case to equivalence with the simple Doppler effect. Now the Doppler effect of a moving scattering particle may be analyzed very simply if we replace the moving scattering particle by a small plane mirror translating with velocity identical to the particle and so orientated as to direct the reflected beam in the direction along which the scattered radiation is to be examined. We can then apply the method of images to the case of the particle.

Referring to Fig. 2, the normal to the small mirror must clearly bisect the angle formed by the incident and scattered rays. Evidently the component of the mirror's velocity parallel to its
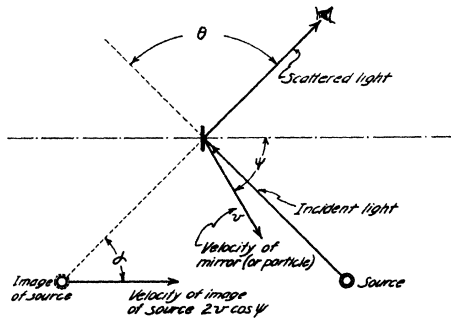

FIG. 2. Doppler effect of a moving scattering particle. The analysis is facilitated by replacing the moving particle by a small plane mirror so orientated as to reflect the radiation along the direction of observation. The motion of the *image* of the source in this mirror can then be considered as producing the observed change in wave-length.

own plane will have no Doppler effect on the reflected beam since this component will impart no motion to the image of the source as seen reflected in the mirror. The effective part of the mirror's velocity is the component velocity resolved normal to the mirror, that is to say, along the bisector between the incident and reflected (or scattered) rays. In Fig. 2 this component is $v \cos \psi$ and the image of the source clearly moves along a direction parallel to this bisecting axis, x, with a velocity $2v \cos \psi$. The reflected (or scattered) ray does not in general coincide with the direction, x,

parallel to which the image of the source moves. We must therefore multiply our image velocity by $\cos \alpha$ or, what is the same thing, $\sin \frac{1}{2}\theta$, to resolve the image velocity along the direction of observation. Thus the Doppler change in wave-length caused by the motion of a scattering particle will be given by the relation

$$\Delta\lambda/\lambda = (2v/c) \sin \tfrac{1}{2}\theta \cos \psi. \qquad (2)$$

It should be noted that the plane of the angle θ need not coincide with the plane of the angle ψ. The formula (2) is thus generally applicable for any direction of the particle velocity in space. Evidently the axis which bisects the angle between the incident and scattered ray (normal to the small mirror in Fig. 2) is a natural reference axis for the problem. When the Doppler change of wave-length becomes an appreciable fraction of the wave-length itself the formulae here given become somewhat modified but there remains a natural reference axis nearly, but not quite, bisecting the angle between incident and scattered rays which is an especially appropriate axis of reference for the problem.

2. Scattering of x-rays by a moving free electron

The analysis is extremely simple for the limiting case when $\Delta\lambda/\lambda \ll 1$ and this case will be treated first. Two simplifying approximations are made. (1) The change in wave-length due to scattering is a negligible fraction of the wave-length itself. (2) Relativity is neglected.

Referring to Fig. 3, the x-axis is taken so as to bisect the angle between the incident and scattered x-ray beams. This angle just mentioned is the supplement of the scattering angle θ. The vectors $h\nu_1/c$ and $h\nu_2/c$ representing respectively the momenta of the incident and scattered quanta of radiation are by approximation (1) sensibly equal. Hence, the change in momentum of the radiation, which is the momentum imparted to the electrons, is given by

$$2(h\nu_1/c) \sin \tfrac{1}{2}\theta \qquad (3)$$

and is directed along the x-axis.

The recoil momentum of the electron will be the vector sum of this acquired momentum and the initial momentum mv which the electron possesses at the instant of scattering. The initial
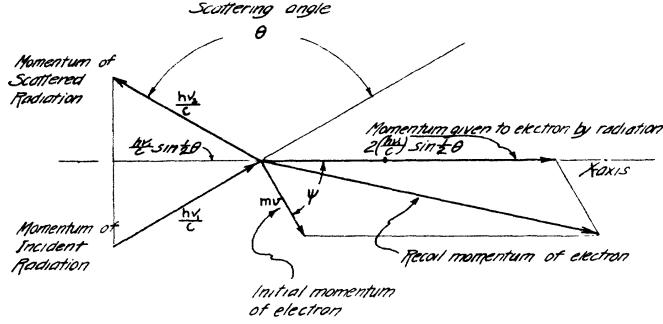
FIG. 3. Diagram of momentum vectors involved in simplified approximate analysis of modified scattering by an initially moving electron. The initial electron momentum is here much exaggerated relative to the momentum of the radiation. The plane of the angle ψ need not coincide with the plane of the angle θ. Complete generality is obtained by rotating the plane of the angle ψ around the x-axis. This in no way affects the analysis here presented.

momentum mv may have any direction *in space* making an angle ψ with our x-axis.

$$(\text{Recoil momentum})^2 = (mv)^2 + 4(h\nu_1/c)^2 \sin^2 \tfrac{1}{2}\theta$$
$$+ 4(mv)(h\nu_1/c) \sin \tfrac{1}{2}\theta \cos \psi. \quad (4)$$

The *recoil energy* is obtained by dividing this equation through by $2m$. Deducting from this result the initial energy $\tfrac{1}{2}mv^2$ possessed by the electron before scattering, we obtain the energy abstracted by the electron from the radiation. Equating this to $h(\nu_1 - \nu_2)$ we obtain

$$h(\nu_1 - \nu_2) = (2/m)(h\nu_1/c)^2 \sin^2 \tfrac{1}{2}\theta$$
$$+ 2v(h\nu_1/c) \sin \tfrac{1}{2}\theta \cos \psi. \quad (5)$$

This is converted into wave-length units by multiplying through by $\lambda/h\nu$ and remembering from approximation (1) that $(\nu_1 - \nu_2)/\nu_1 = (\lambda_2 - \lambda_1)/\lambda_1$. The change in wave-length due to scattering thus turns out to be

$$\lambda_2 - \lambda_1 = (2h/mc) \sin^2 \tfrac{1}{2}\theta + (2v/c)\lambda \sin \tfrac{1}{2}\theta \cos \psi. \quad (6)$$

The first term represents the well-known Compton shift, while the second term is the modification in the shift caused by the electron's initial velocity. Call this term l. Reference to Eq. (2) shows that this term may quite appropriately be regarded as a *Doppler shift caused by the component of the electron's* initial velocity along x. Since the electron may move in any direction, $\cos \psi$ can take all values between $+1$ and -1 and l can vary from $-2\beta\lambda \sin \tfrac{1}{2}\theta$ to $+2\beta\lambda \sin \tfrac{1}{2}\theta$.

Thus the Compton line acquires a breadth

$$4\beta\lambda \sin \tfrac{1}{2}\theta, \quad (7)$$

where $\beta = v/c$ for electrons moving in random directions and each having a speed v.

We now consider the more elaborate analysis of the general case of scattering by a moving free electron when the change in wave-length is not a negligible fraction of the wave-length itself and
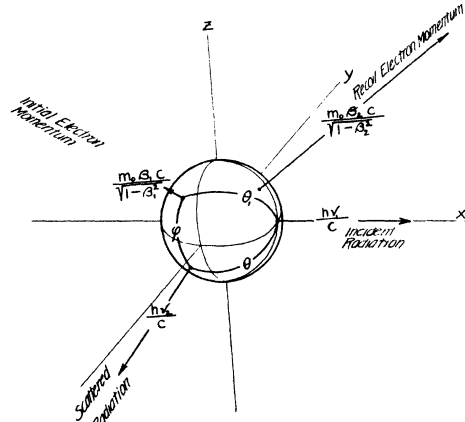

FIG. 4. Illustrating the various angles and vectors involved in modified scattering by an electron possessing initial momentum. The initial electron momentum is exaggerated. The vectors are shown radiating from a sphere at the origin on which the angles between vectors appear as arcs of great circles to aid in visualizing the diagram in three dimensions.

when the formulae of special relativity are applied.

Referring to Fig. 4, the primary radiation is taken as travelling in the positive x-direction. θ is the angle of scattering; ν_1 is the initial frequency; $\beta_1 c$ the speed of the electron before scattering; a_1, b_1, c_1, the direction cosines of its velocity; θ_1 is the angle between the initial electron momentum and the initial radiation momentum so that $a_1 = \cos \theta_1$; ν_2 is the frequency of the scattered quantum and its direction of propagation has the direction cosines p, q, r making an angle ϕ with the initial velocity of the electron and an angle θ with OX. Evidently $\cos \phi = a_1 p + b_1 q + c_1 r$, $p = \cos \theta$. The recoiling electron has a final speed $\beta_2 c$ in the direction defined by the cosines a_2, b_2, c_2.

The following four equations express, respectively, the conservation of energy and of the three components of linear momentum before and after the scattering process:

$$h\nu_1 + m_0 c^2/(1-\beta_1{}^2)^{\frac{1}{2}}$$
$$= h\nu_2 + m_0 c^2/(1-\beta_2{}^2)^{\frac{1}{2}}, \qquad (8)$$

$$h\nu_1/c + \{m_0\beta_1 c/(1-\beta_1{}^2)^{\frac{1}{2}}\}a_1$$
$$= (h\nu_2/c)p + \{m_0\beta_2 c/(1-\beta_2{}^2)^{\frac{1}{2}}\}a_2, \quad (9)$$

$$\{m_0\beta_1 c/(1-\beta_1{}^2)^{\frac{1}{2}}\}b_1$$
$$= (h\nu_2/c)q + \{m_0\beta_2 c/(1-\beta_2{}^2)^{\frac{1}{2}}\}b_2, \quad (10)$$

$$\{m_0\beta_1 c/(1-\beta_1{}^2)^{\frac{1}{2}}\}c_1$$
$$= (h\nu_2/c)r + \{m_0\beta_2 c/(1-\beta_2{}^2)^{\frac{1}{2}}\}c_2. \quad (11)$$

Eliminating a_2, b_2, c_2 and β_2 and letting $\alpha = h\nu_1/m_0 c^2$, we obtain on solving for the change in wave-length

$$\lambda_2 - \lambda_1 = \frac{\beta_1(\cos \theta_1 - \cos \phi)}{1 - \beta_1 \cos \theta_1}\lambda_1 + \frac{2\alpha\lambda_1 \sin^2 \frac{1}{2}\theta}{1 - \beta_1 \cos \theta_1} \quad (12)$$

where the second term accounts for the simple Compton shift and the first term represents the Doppler modification caused by the electron's initial speed $\beta_1 c$.

As we are particularly interested in the *breadth* of the shifted line we define a wave-length coordinate l, where $l = \lambda_2 - \lambda_1 - 2\alpha\lambda_1 \sin^2 \frac{1}{2}\theta$ so chosen that l has its origin at the "center" of the shifted line (shifted position for scattering by free *initially stationary* electrons) and measures the wave-length deviation given by the first term of

the right-hand member of Eq. (12). Then

$$l = \frac{\lambda_c \cos \theta_1 - \lambda_1 \cos \phi}{1 - \beta_1 \cos \theta_1}, \qquad (13)$$

in which λ_c is the Compton shifted wave-length for the simple case of an initially stationary electron $\lambda_c = \lambda_1 + 2\alpha\lambda_1 \sin^2 \frac{1}{2}\theta$.

Eq. (13) can be much simplified by describing the direction of the initial electron momentum in terms of a new angle ψ measured from a reference axis taken in the direction of the change in momentum which the radiation would suffer for the simple Compton case of an initially stationary electron scattering radiation at angle θ.

In Fig. 5 let OA be the direction of the incident quantum, OB the direction of the scattered quantum, OC the direction of the electron's
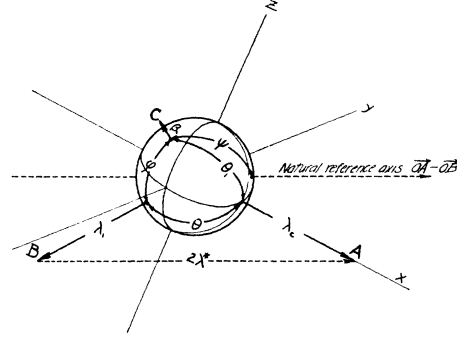

FIG. 5. Illustrating the definition of the "natural" reference axis and of the angle ψ. It should be emphasized that λ_c is the simple Compton shifted wave-length for the case where vector C vanishes ($\beta_1 = 0$) and that since λ_c is constant for a given primary wave-length and scattering angle, the direction of the natural reference angle is constant. Note that λ_c is taken along the *incident* direction and λ_1 along the scattered direction. This inversion is caused by the fact that the momenta are inversely as the wave-lengths.

initial velocity. Lay off the vector OA equal in length to λ_c, the vector OB equal in length to λ_1 and the vector OC equal in length to β_1. We define a new wave-length, λ^* represented to the same scale as λ_1 and λ_c by half the distance AB. Now note that the numerator of Eq. (13) can be represented in terms of the vectors of Fig. 5 (designated by their terminii) as the difference of two scalar products, $C \cdot A - C \cdot B$, or, what is equivalent, $C \cdot (A - B)$.

The vector whose length is $2\lambda^*$ is precisely $(A-B)$, hence if ψ is the angle between OC and AB we rewrite Eq. (13) as follows

$$l = [\cos\psi/(1-\beta_1\cos\theta_1)]2\beta_1\lambda^*, \quad (14)$$

where

$$2\lambda^* = (\lambda_c{}^2+\lambda_1{}^2-2\lambda_c\lambda_1\cos\theta)^{\frac{1}{2}}. \quad (15)$$

The denominator of Eq. (14) is nearly unity in most practical cases. Thus it is evident that the wave-length deviation, l, from the simple Compton shift caused by an initial velocity, $\beta_1 c$, of the scattering electron (instead of zero velocity) is proportional to the projection, $\beta_1\cos\psi$, of the electron's initial velocity along the direction of the vector representing the change in momentum which the radiation would suffer if scattered by an initially stationary electron through the scattering angle θ. This direction is the analogue of the axis x of Fig. 3 and indeed very nearly coincides with it.

This natural reference axis appropriate to the problem is thus a stationary axis in space independent of the direction of the electron's initial motion and the projection of the electron's velocity upon it can have either the positive or negative sign according to the sign of $\cos\psi$. Thus the extreme values of l are given (if $\beta_1{}^2$ be considered negligible compared to unity) by the inequality

$$-2\beta_1\lambda^*+2\beta_1{}^2\lambda^* \sin\tfrac{1}{2}\theta \leq l \leq 2\beta_1\lambda^*$$

$$+2\beta_1{}^2\lambda^* \sin\tfrac{1}{2}\theta \quad (16)$$

or if the first power of β_1 be considered negligible compared to unity

$$-2\beta_1\lambda^* \leq l \leq 2\beta_1\lambda^*. \quad (17)$$

In either case, therefore, l can vary over the wave-length range

$$\Delta\lambda = 4\beta_1\lambda^* \quad (18)$$

for electrons of initial speed β_1 and all possible directions of motion.

It is evident from Eq. (15) that when λ_c approaches equality with λ_1 the wave-length λ^* approaches the value $\lambda_1\sin\tfrac{1}{2}\theta$. Thus Eqs. (14) and (18) of the exact theory are seen to reduce to Eqs. (6) and (7) of the approximate theory when the wave-length change can be neglected in comparison to the wave-length itself.

Before considering the spectral distribution to be expected over the range defined by Eqs. (7) and (18), it is well to summarize the results of the theory so far. It appears that *an ensemble of electrons all possessing the speed βc and isotropically distributed in space as to direction should, in scattering an initially sharp spectral line of wave-length, λ, introduce a broadening in the line which measured in wave-length units should be approximately proportional jointly to the primary wave-length and to the sine of half the scattering angle.*

It is worthy of note that, as the primary wave-length tends toward the limit zero, the broadening under discussion does not vanish but approaches a residual value

$$\operatorname*{Lim}_{\lambda\to 0}\Delta\lambda = 2\beta\,\frac{h}{mc}\,(1-\cos\theta). \quad (19)$$

This can be readily seen from the expression for λ^* as a function of λ_1 which is

$$\lambda^* = \lambda_1\sin\tfrac{1}{2}\theta\left[1+\frac{k}{\lambda_1}+\tfrac{1}{4}\frac{k^2}{\lambda_1{}^2}\frac{1}{\sin^2\tfrac{1}{2}\theta}\right]^{\frac{1}{2}}, \quad (20)$$

in which $k = (2h/mc)\sin^2\tfrac{1}{2}\theta$.

The course of λ^* as a function of λ_1 is seen from Eq. (20) to be not quite linear. However, the deviation from linearity is very slight indeed. Fig. 6 shows a plot of λ^* as a function of λ_1 for several different scattering angles. The dependence of λ^* on the scattering angle, θ, is also shown in Fig. 25 computed for a wave-length of 710 x.u. The curve differs but little from the function $\lambda\sin\tfrac{1}{2}\theta$.

3. Spectral distribution for an ensemble of moving free electrons

From the foregoing considerations it is evident that the distribution of the velocities or momenta of an ensemble of free electrons will determine the spectral distribution of the modified and broadened line which will result when these electrons scatter initially monochromatic radiation under a well-defined scattering angle. We describe the distribution of electron momenta in a momentum space in which the three coordinate axes represent the three cartesian coordinates p_x, p_y, p_z, of the momentum of any electron. The momentum of any electron is then a vector from the origin of this space to the point p_x, p_y, p_z. The distribution of the points p_x, p_y, p_z corresponding to each

and every electron throughout this space is then descriptive of the electron momentum distribution.

Let us start with a simple momentum distribution consisting of electrons whose momentum vectors all terminate in a spherical shell of thickness dp and radius p, corresponding to an electron velocity $\beta c = p/m$, the vector terminii being uniformly dense all over the surface of the sphere,
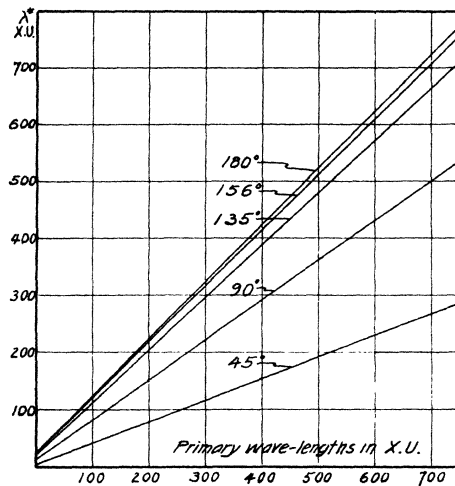

Fig. 6. Illustrating the dependence of λ^* on primary wave-length for several scattering angles. The curves deviate only very slightly from straight lines. As long as the unmodified scattering is a negligible fraction of the total scattering these curves also illustrate the behavior of modified line breadth as a function of primary wave-length for the scattering angles indicated. λ^* is about 35 times as great as the breadth at half maximum for the case of graphite.

i.e., an isotropic distribution of momentum. Let us choose the polar axis of this sphere so as to coincide with the direction of the natural reference axis referred to in the previous analysis, i.e., nearly in the bisector of the angle formed by the incident and scattered ray. We recall that it is the component of momentum of each electron resolved along this axis which determines the spectral shift which will occur when this electron scatters the radiation. The angle ψ of the previous section is then the colatitude angle measured on this sphere. The total intensity scattered in the range dl with a given shift, l, away from the

spectral position corresponding to free stationary electrons will be proportional to the number of electrons having a momentum component capable of giving this shift.

The fraction of all electrons whose momenta lie in the range $d\psi$ at angle ψ will evidently be the area of the zone between ψ and $\psi + d\psi$ divided by the area of the sphere. That fraction is

$$P(\psi)d\psi = \tfrac{1}{2} \sin \psi d\psi. \tag{21}$$

The probability $P(l)dl$ of a given deviation l in the range dl is then to be obtained by eliminating ψ and $d\psi$ between Eqs. (14), the derivative of (14) and Eq. (21). This operation is very simple if we set the denominator in Eq. (14) equal to unity. This amounts to neglecting β in comparison to unity. The result is

$$P(l)dl = (4\beta\lambda^*)^{-1}dl. \tag{22}$$

For $\lambda^* = 740$ x.u. and $l = 25$ x.u. the error committed is about 3 percent. The spectral intensity distributions actually observed have breadths which fall well below this range so that the application of formula (22) to the prominent parts of the line structure introduces wholly negligible errors. It will be seen below that the predominant values of β obtained by analyzing the spectral line structure turn out to be less than 0.01.

Now from Eq. (22) since the right-hand member is independent of l it is evident that all deviations, l, are equally probable within the limits placed by inequalities (16) or (17). Outside these limits no shift can occur. Hence (see Fig. 7),
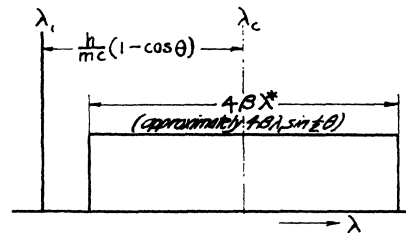

Fig. 7. Spectral distribution of modified scattered x-radiation for the ideal case of a monochromatic primary ray scattered by an assembly of electrons all of momentum $m\beta c$ isotropically distributed as to direction. The distribution is symmetrically disposed about the wave-length λ_c, the shifted wave-length for initially stationary electrons. The distribution has a breadth $4\beta\lambda^*$ proportional to the common speed of the electrons and is bounded by sharp discontinuities on both sides. Between these limits the distribution is uniform.

a good approximation to the spectral distribution contributed by our isotropically directed ensemble of electrons of speed βc will be a rectangular spectral distribution of breadth $4\beta\lambda^*$, and of area proportional to the population of the speed class β in the range $d\beta$. (This distribution is not quite centered on the shifted position for stationary electrons but as can be seen from inequality (16) is displaced toward longer wave-lengths by a slight amount $2\beta_1{}^2\lambda^* \sin \frac{1}{2}\theta$. This shift is wholly inappreciable for values of β of importance in the experimental case, however.)

We now pass to the more general case of an ensemble of electrons whose distribution in momentum space is any function of the radius but isotropic as to direction. Let the radial distribution be represented by a function $\Phi(\beta)$ such that $\Phi(\beta)d\beta$ is proportional to the number of free electrons whose speeds lie in the range $cd\beta$ at the value $c\beta$. Each shell in momentum space will contribute its rectangular spectral distribution of area proportional to the electron population of that shell so that the line structure in this case is to be thought of as built up out of an assemblage of rectangles of infinitesimal height each having a breadth equal to $4\beta\lambda^*$ and an area proportional to the population of the shell of radius $mc\beta$. For convenience in adding spectral intensities the rectangles must of course be superposed in order of decreasing breadth, that is to say, decreasing values of β. Referring to Fig. 8, the curve $\Phi(\beta)$ on
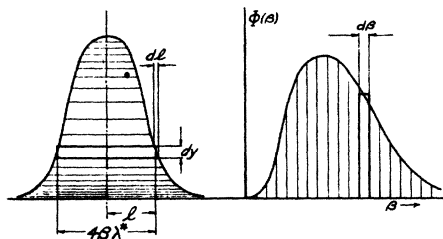

Fig. 8. Illustrating the relation between spectral intensity distribution of shifted radiation (left) and population of electron speed (or momentum) states (right). Each elementary rectangle on the left is equal in area to a rectangle on the right while the spectral breadth $4\beta\lambda^*$ of each rectangle on the left is proportional to the abscissa β of the rectangle on the right.

the right represents the electron population distribution over the states or speeds β, while the

curve on the left represents the spectral distribution across the modified line which will result from such a distribution of speeds. The elementary rectangular area $2l dy$ in the left-hand curve is to be kept proportional to the elementary rectangular area $\Phi(\beta)d\beta$ in the right-hand curve. If the constant of proportionality is k we can express the differential equation of the line structure curve in terms of the speed distribution function thus

$$-2l dy = k\Phi(\beta)d\beta, \qquad (23)$$

since the half breadth of each rectangle is $l = 2\beta\lambda^*$, we can replace $d\beta$ by $dl/2\lambda^*$ and β by $l/2\lambda^*$. Dividing Eq. (23) by $-2l$ and integrating from $y=0$, $l=\infty$ to $y=y$, $l=l$, we obtain the equation of the modified line structure curve for continuous functions which vanish as $l\to\infty$

$$y = -k\int_{l=\infty}^{l=l} l^{-1}\Phi(l/2\lambda^*)dl. \qquad (24)$$

Furthermore, if in Eq. (23) we substitute $dl/2\lambda^*$ for $d\beta$ and divide through by dl we obtain $\Phi(\beta)$ in terms of the line structure curve where K is another constant of proportionality

$$\Phi(\beta) = \Phi(l/2\lambda^*) = Kl dy/dl. \qquad (25)$$

Eq. (24) permits us to take hypothetical electron momentum distributions and compute the resulting shifted line structure for comparison with the observed shifted line structure. Eq. (25) permits us to compute from an observed shifted line structure the electron momentum distribution which must have caused it.

We have thus far only considered distributions in momentum space possessing spherical symmetry, i.e., isotropic as to direction. It is extremely easy to secure such a directionally isotropic distribution of electron momenta, for it is sufficient to reduce the scattering material to a fine powder which can be contained in a cellophane holder so thin as to contribute inappreciably to the scattering. This procedure was followed for a beryllium scatterer with the multicrystal spectrograph.

The only other type of momentum distribution which need be discussed is one in which the component p_z (directed along the natural reference axis nearly bisecting the angle between incident and scattered beams) vanishes nearly or com-

pletely while the components, p_y, p_z, take any values whatever. In such a momentum distribution the momentum vectors would be all very nearly parallel to the y, z plane and their terminii would lie entirely inside a thin flat slab parallel to the y, z plane and closely coinciding with it. The absence of any appreciable x-component of momentum would thus give a *narrow sharp shifted line* and this sharpness would be unaffected by the y and z components of momentum. We have never observed anything of this sort although an elaborate experiment[7] was devised in an effort to reveal the presence of such preferentially directed momenta. Space does not permit a complete description of this experiment which was performed with a scatterer of Ceylon graphite. This crystal occurs in small thin flat flakes and its magnetic and mechanical properties are exceedingly anisotropic. It was thought possible that a fairly populous isolated class of electrons in these crystals might have their momenta chiefly parallel to the plane of the flakes. Blocks of this graphite were built up in which the crystals stuck together with an exceedingly small amount of binding gum had their planes in mutual parallelism. The scatterer was built up of these blocks so orientated that the normals to the planes of the flakes bisected the angle formed by the primary and scattered x-ray beams. No detectable sharpening of the peak of the modified line was observed. No other orientation of the blocks with respect to the x-rays was tried, for considerations of symmetry give no hope of finding an effect in other positions.

4. Variation of modified line breadth with scattering angle and primary wave-length

It is important to note that *for any constant momentum distribution whatever* the breadth of the shifted line will depend on the scattering angle and on the primary wave-length, the form of this functional dependence being given by λ^*, see Fig. 6. Roughly the breadth should be proportional to the primary wave-length and to the sine of half the scattering angle as we have already pointed out. There is no ambiguity about the breadth of a rectangular spectral distribution such as is shown in Fig. 7 but real Compton lines

[7] DuMond, Kirkpatrick and Alden, Phys. Rev. [2] 40, 165 (1932).

resemble more nearly Fig. 8, the scattering electrons being distributed without doubt over a wide range of momenta. We shall arbitrarily define the "breadth" of such "lines" as the breadth measured in wave-length units across the spectral distribution curve at a point where the intensity has fallen to half its maximum value. The elementary rectangle at this point is contributed by a certain speed class of the scattering electrons which we can for brevity call the class β_i. Now if we vary either the primary wave-length or the scattering angle so as to obtain a new value of λ^* *all* the elementary rectangles going to make up the line structure will vary in spectral breadth in the same way and hence that particular elementary rectangle which occurred at the point half-way between maximum and zero intensity and was contributed by the speed class which we called β_i will still occur at this same relative height. Thus the variation in the breadth of the "line" measured at half maximum height will be exactly the variation due to λ^* so long as the momentum distribution of the free electrons remains unchanged.

Experiments must, of course, be made on solid bodies as scattering materials and the last statement is then only approximately true because of the varying degree to which unmodified scattering plays a part as the scattering angle and primary wave-length are changed. The more strongly bound electrons (which also have the higher momenta) will then not contribute to the modified scattering but to the unmodified scattering, and there will, therefore, be a slight selection in favor of lower momenta for modified scattering when the unmodified line is relatively strong. This selective effect is of very little importance, however, if we restrict our study to cases where the unmodified line is weak relative to the modified line. In the studies here described we have been careful to do this.

We thus have a most valuable check to test whether our theoretical interpretation is truly applicable to the broad modified lines actually observed, for we have only to vary the primary wave-length and the scattering angle and see whether the breadth of the observed lines follows the predicted behavior. It if does we shall have the strongest evidence that the breadth of the modified line is interpretable as a Doppler

broadening caused by the chaotic electron momenta in atoms.

5. Scattering by bound electrons

The difficulties of a rigorous analysis of the problem of modified scattering by bound electrons are very considerable. We shall mainly confine ourselves here to a discussion of the order of magnitude of the errors introduced by applying the foregoing theory for free electrons with initial momentum to the case of scattering by bound electrons.

Before the advent of the wave mechanics and quantum mechanics, Jauncey[4] regarded the process whereby a bound electron scattered a photon of radiation as an impulsive collision between two particles. The duration of this process he supposed to be so brief that no appreciable change in the potential energy of the electron occurred in the interval. The exchange of momentum and energy between the photon and the electron then occurred exactly as though the electron were a free electron with the same momentum as that of the bound electron in its orbit. With these assumptions the foregoing theory for the scattering by free electrons could be applied without modification, save for one restriction imposed by the conservation of energy. This restriction has been discussed both by Compton in his treatise on x-rays and electrons, and by Jauncey[4] who first used it as the explanation of the mechanism of coherent or unmodified scattering. According to the impulsive picture of the scattering process just mentioned the energy imparted to the electron (and hence lost by radiation) is *subsequently* used, at least in part, to effect the electron's escape from the atom. A *free* electron with specified initial momentum scattering radiation of wavelength λ under a specified angle will receive a definite recoil energy according to the laws of conservation of energy and momentum as set forth in our theory. Jauncey assumed that a *bound* electron having the same specified momentum will, under the same specified conditions, receive this same recoil energy if, and only if, this recoil energy exceeds the binding energy. If this recoil energy is less than the binding energy the electron will behave as though its mass were the mass of the entire atom and the laws of conservation of momentum and energy will then require

an entirely negligible change of wave-length. This accounts for the unmodified scattered line. A third possibility not mentioned in Jauncey's discussion should also be noticed. The energy imparted to the electron by the radiation may be exactly equal to the work required to raise the electron from its initial energy level to some discrete unfilled energy level in the atom. In this case a *sharp line* of longer wave-length than the primary radiation should appear in the scattered spectrum. We should thus expect the contribution of each electron shell in the scattering atom to the broad modified line to be cut off more or less sharply on the short wave side at a wavelength where the shift from the primary wavelength corresponds to an energy transfer equal to the ionization energy of that shell and in this suppressed region between the cut-off edge and the primary line there should appear a spectrum of sharp lines caused by electron transitions to discrete levels. These lines predicted long ago by Smekal[8] would be called today Raman lines. Their existence[9] has not been firmly established by observation, probably due to their very weak intensity, as predicted by quantum mechanics.

The ideas of Jauncey as to the mechanism of unmodified scattering led to a fairly accurate quantitative prediction of the ratio of modified to unmodified total intensity and hence must have contained important elements of truth. However, no indication of the spectral discontinuities which it predicts has as yet been observed.

We can, by classical quantum considerations, obtain a rough idea of the deviation from formulae (6) or (14) which will occur for the case of a bound electron as follows: We assume the bound electron to be initially in a state whose energy is $W_1 = T_1 + V_1$ (a negative energy state). The final state of the recoil electron corresponds to an energy $W_2 = T_2$ (a positive energy state).

Let us assume (as an opposite extreme to the impulsive assumption in Jauncey's theory) that $h\nu_1 - h\nu_2 = W_2 - W_1$. From Eq. (4) for free electrons dividing by $2m$ we obtain an approximation to $W_2 = T_2$ so that

$$h\nu_1 - h\nu_2 = W_2 - W_1 = \tfrac{1}{2}mv_1{}^2 + (2/m)(h\nu_1/c)^2 \sin^2 \tfrac{1}{2}\theta$$
$$+ 2v_1(h\nu_1/c) \sin \tfrac{1}{2}\theta \cos \psi - W_1.$$

[8] Smekal, Naturwiss. 11, 873 (1923).

[9] Davis, Phys. Rev. [2] 32, 33 (1928).

Now multiply by $\lambda/h\nu_1$ and replace $\nu_1-\nu_2/\nu_1$ by $\lambda_2-\lambda_1/\lambda_1$. This gives

$$\lambda_2-\lambda_1=\lambda_1\{(T_1-W_1)/h\nu_1\}$$
$$+(2h/mc)\sin^2\tfrac{1}{2}\theta+(2v/c)\sin\tfrac{1}{2}\theta\cos\psi. \quad (26)$$

This is seen to differ from formula (4) only in the first term of the right-hand member which is essentially a fraction of the primary wave-length equal to the quotient of the initial potential energy of the electron divided by the quantum energy of the incident radiation. In most practical cases this term is very small compared to either of the other two terms of Eq. (26). For example, in the case of molybdenum K radiation scattered by the L electrons of carbon at large angles the term amounts to less than 1 x.u., whereas the second and third terms are of the order of 50 x.u. and 20 x.u., respectively. This term is more appreciable for the K electrons but these latter contribute relatively little to the prominent parts of the modified line. This term has an analogue in the quantum mechanical treatment of the problem of scattering by bound electrons as we shall presently see. It seems improbable that a correction of this type for the binding energy of the electron can be large because the effect of such a term is to increase the shift of the center of the broadened modified line toward longer wave-lengths than those predicted by the Compton shift formula (since the average value of T_1-W_1 is a positive quantity) and no appreciable deviation of this type appears in the experimental observations here reported. In terms of the *shift*, $\delta\lambda=\lambda_2-\lambda_1$, the above correction term is $\delta\lambda$ (potential energy/recoil energy).

6. Remarks on quantum mechanical theory of modified scattering by bound electrons

The difference between the quantum mechanical aspect of this problem and the treatment given above is more apparent than real. Wentzel[10] has given a theory of scattering according to which the modified line is a small continuous spectral distribution ascribed to scattering electrons whose initial state is a discrete negative energy level and whose final state is one of the continuum of positive energy levels (recoil elec-

trons). It turns out from this theory that the maximum of this modified continuous distribution will occur at a shifted position precisely the same as that given by the Compton formula and the breadth of this maximum will be proportional to a term $(2mE)^{\frac{1}{2}}$ *representing the momenta of the bound electrons*. Indeed the analytic condition determining the position of the maximum turns out to be formally identical to the results of the application of the laws of conservation of momentum and energy to the scattering process.

In Wentzel's last paper on this problem[11] it will be noted that his quantity $n=\alpha/2k$ (Eq. (19), page 357) is the ratio of the reciprocal Bohr radius $(\alpha=4\pi^2me^2h^{-2})$ to the parameter $2k$ describing the final state of the recoil electron. The equation $W_k=h^2k^2/(8\pi^2m)$ (page 350) gives the final energy W_k of the recoil electron. Thus $\alpha=2\pi h^{-1}p_0$ where p_0 is the momentum of the electron in the first classical Bohr orbit and $k=2\pi h^{-1}p_k$ where p_k is the momentum of the recoil electron. As Wentzel points out $n^2\ll1$, and hence can be neglected in his Eq. (29), page 362. This is analogous to the negligibility of the term in the preceding section (our Eq. (26)).

Wentzel's final formula for the shape of the modified line as scattered by a bound electron in the ground state of hydrogen is given in his Eq. (33), page 366. The maximum occurs at the Compton shifted position and the term α accounts for the "breadth" of the distribution. If this is compared with the formula of the author[12] for $y_{1,\,0}$, the two will be found identical save for a normalizing constant. The author's formula was derived, however, by treating the problem as though the electrons in the atom were essentially free electrons scattering the radiation and broadening the shifted line in virtue of the Doppler effect of their initial velocities in accord with the simple theory set forth in this paper, these initial velocities or momenta being distributed according to the probability distribution required by quantum mechanics. *We can safely conclude therefore that when Wentzel's n^2 is small, that is,*

[10] G. Wentzel, Zeits. f. Physik **43**, 1 (1927); **43**, 779 (1927); **58**, 348 (1929).

[11] G. Wentzel, Über den Rückstoss beim Comptoneffekt am Wasserstoffatom, Zeits. f. Physik **58**, 348–367 (1929).

[12] Jesse W. M. DuMond, Compton Modified Line Structure and its Relation to the Electron Theory of Solid Bodies, Phys. Rev. [2] **33**, 651 (1929), (near the top of page 651).

when the binding energy of the electrons is small compared to the recoil energy, the author's interpretation of the breadth and structure of the shifted radiation is in no way discordant with quantum mechanics and furnishes a valid method of studying the distribution of linear momentum in atoms.

Now, as a matter of fact, there is a practical reason why only just these cases of relatively weak binding can be studied. It turns out experimentally that unless one employs the K radiation from a target material of *very much higher* atomic number than the atomic number of the scattering body the scattered radiation is too weak to permit a study of its spectral distribution. This is because the fluorescent absorption so limits the depth to which rays penetrate below the surface of the scattering body that, unless the radiation is "hard" and the scattering body of low atomic number, an insufficient volume of scattering atoms is brought into play.

It is essential to note that the observation of the internal linear momenta in atoms by means of the Doppler modification impressed on scattered radiation in the way to be described below is in no way a violation of the famous uncertainty principle of Heisenberg. This is because the experiment places no restriction on the *position* of the electrons whose momenta are observed. It would seem, therefore, valid to interpret the momentum distributions obtained as actually representing the probability of observing a momentum p in the range dp.

The author's interpretation of the broadened modified line as essentially a picture of the momentum distribution of the electrons in the atom is no more objectionable than the interpretation put upon x-ray diffraction and scattering experiments in terms of electron space density distributions in crystals or in free atoms. In fact, the two cases are exact parallels. Compton and others

have measured the distribution of scattered intensity of x-rays as a function of the scattering angle both for crystals and gases. These results are then interpreted by analytical methods analogous to those used for diffraction problems in optics and the results are discussed as the "radial distribution of electron density" in an atom or the distribution of electron density in a crystal lattice. In quantum mechanics this means a space eigenfunction $|\psi|^2$. The author measures the *spectral distribution* of modified scattered radiation and interprets these results as the distribution of the electrons in momentum space. In quantum mechanics this means a nomemtum eigenfunction $|\varphi|^2$. It would seem that the resort to somewhat pictorial language is, in his case, quite as justified (though not as familiar) as in the diffraction case. There is, in the opinion of the author, altogether too much tendency to make an unnecessary mystery of quantum mechanics and to refuse to look at its approximate interpretations in familiar terms. No danger is involved in such a procedure if one is honest in remembering the qualifying conditions which render the approximation valid. Much of the heuristic value of physics grows out of this very process of splitting the unity of natural phenomena into separate understandable "effects."

7. Computation of theoretical momentum distributions for comparison with experiment

Podolsky and Pauling[3] have derived an expression for the momentum distribution of electrons in hydrogen-like atoms by means of a Dirac transformation from the position eigenfunctions. Their expression for the probability that the electron shall have a momentum whose absolute value lies in the range between P and $P+dP$ is $W_{nl}(P)dP$

$$W_{nl}(P) = \frac{a_0}{Zh} \frac{2^{4l+6}n^2(l!)^2(n-l-1)!}{(n+l)!} \frac{\zeta^{2l+2}}{(\zeta^2+1)^{2l+4}} \left[C_{n-l+1}^{l+1} \left(\frac{\zeta^2-1}{\zeta^2+1} \right) \right]^2. \tag{27}$$

Here a_0 is the radius of the first Bohr orbit, Z the effective atomic number, n and l the quantum numbers, $\zeta = nh(2\pi\mu e^2 Z)^{-1}P$ and the expression in brackets is one of the Gegenbauer C functions tabulated below for a few values of n and l

Values of $C(x)$

	$l=0$	$l=1$	$l=2$	$l=3$
$n=1$	1			
$n=2$	$2x$	1		
$n=3$	$4x^2-1$	$4x$	1	
$n=4$	$8x^3-4x$	$12x^2-2$	$6x$	1

To approximate the momentum distribution in an atom such as carbon the formula (27) is weighted in proportion to the number of electrons in each state (n, l) and a mean effective atomic number is substituted for Z to allow for screening. The distribution curves for all the states are then simply added. The choice of screening constants is a delicate matter. Pauling, Zener and Slater have each treated this subject.[13] At best an approximation of this type is more or less rough and can only be expected to give an idea as to whether the experiment gives momenta of the order of magnitude to be expected theoretically.

In particular the momenta derived in such a way are likely to be in error on account of the effect of neighboring atoms. Formula (27) applies strictly to an atom free from the disturbing effect of neighbors. In solids which must be used as scattering bodies the proximity of the atoms tends to require higher velocities for the outer electrons. This is discussed in more detail in a later section.

C. EXPERIMENTAL EVIDENCE

8. Evidence for the broadening of the modified line

The chief experimental difficulty in the study of the spectrum of modified scattered x-radiation is the very low intensity of the scattered radiation. This difficulty is accentuated if the requirement of a sharply defined scattering angle is imposed for there are no x-ray lenses available to collect a large solid angle of radiation from the source and transform it into a parallel beam so as to permit of scattering under a definite angle. The early experimental work on modified scattering was performed with scattering angles whose inhomogeneity was of the order of many degrees. Now since the shift depends on the scattering angle according to the formula

$$\text{Shift} = (2 \ h/mc) \sin^2 \tfrac{1}{2}\theta \qquad (28)$$

it is evident that an inhomogeneous scattering angle will broaden the modified line. This spurious experimental broadening will be most accentuated for scattering angles of 90° and will

diminish as we approach angles of zero and 180° as can readily be seen by reference to Fig. 9. The small shift and the difficulty of screening off the direct beam make the region near zero scattering angle undesirable for study. There remains the region of large scattering angles near 180° which is very favorable and permits of fairly inhomogeneous scattering angles without much consequent increase in modified line breadth.

From the first it was suspected that the modified lines observed were broader than could be accounted for by the inhomogeneity of the scat-
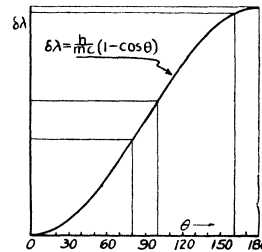

FIG 9. Illustrating the spurious breadth introduced by a given inhomogeneity of scattering angle at different scattering angles.

tering angle. H. M. Sharp[14] was the first to test this point in an experiment whose chief purpose was to obtain an accurate measurement of the shift. His scattering angle was about 169° with an inhomogeneity of about 5°. The reproduction of his spectrum shows the modified line distinctly broader than either the unmodified line or the fluorescent zirconium line (produced on the same negative by replacing the original paraffin scatterer with a zirconium radiator). The breadth is far too great to be accounted for by the combined effect of his inhomogeneity of scattering angle and the rather broad slit he used. Although Sharp made no mention of this distinct broadening in his paper the conclusion from his reproduced spectrum and from his microphotometer curves taken on his original negative is inescapable.

In spite of this evidence the reality of the broadening of the modified line was not definitely accepted for a very long time [15] and indeed the

[13] Pauling, Proc. Roy. Soc. A114, 181 (1927); Zener, Phys. Rev. [2] 36, 51 (1930); Slater, Phys. Rev. [2] 36, 57 (1930).

[14] H. M. Sharp, Phys. Rev. [2] 26, 691 (1925).

[15] See remarks by A. H. Compton in his treatise, X-Rays and Electrons, p. 293, in discussing a spectrum by Ross.
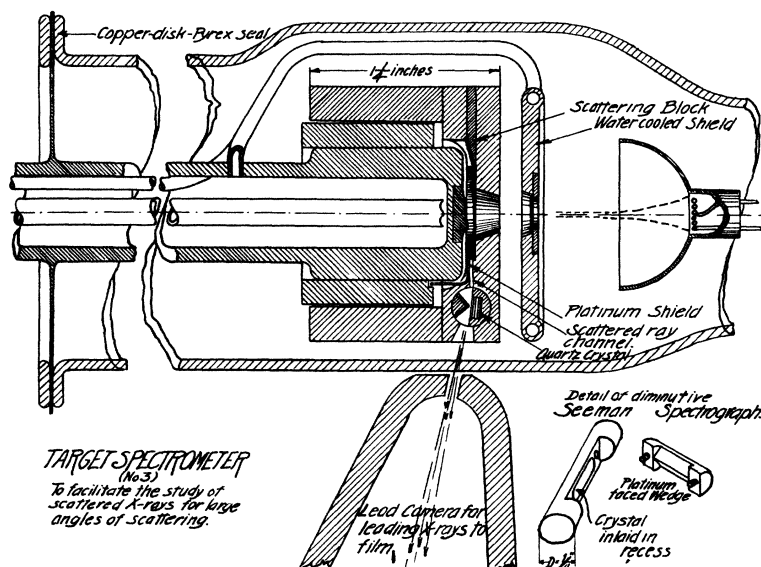
FIG. 10. Design of x-ray tube with scattering body and quartz Zeeman spectrograph
supported on target.

unmistakable evidence of the author and his co-workers came at a time when three papers[16, 17, 18] had just previously been published reporting very narrow modified lines. It is only fair to state that the chief purpose in the three papers was to study the *shift* and not the breadth however.

The author's first attempt[19] to definitely establish the reality of the large broadening of the modified line and to study the structure of this broadening was made by means of an especially designed x-ray tube provided with a small Zeeman wedge spectrometer in a housing supported on the target inside the tube. The design was such as to afford as large a scattering angle as possible to reduce the spurious modified line breadth caused by the inhomogeneity of scattering angle. Fig. 10 shows the "target spectrometer" in cross section. The anti-cathode was a General Electric water-cooled target with molybdenum button. This button projected slightly

beyond the copper (which had been turned off to a slight depth in the lathe) and the end of the projecting button was beveled so as to face toward the scattering block and away from the crystal. This facilitated the passage of primary radiation to the scatterer and prevented it from striking the crystal from which by nonselective scattering it could easily fog the photographic film. The cylindrical box surrounding the anti-cathode contained the scatterer and the small Zeeman wedge spectrograph. Great care was taken in the internal design of the box to insure that the radiation analyzed by the spectrograph came only from the scattering body. A water-cooled shield between the box and the cathode was found necessary to prevent stray electron impacts from overheating the box. Before enclosing the anti-cathode and its box in the x-ray tube the quartz crystal and wedge in the small cylindrical container were carefully orientated to such an angle that the region of the spectrum studied came exactly from the center of the scattering substance. This was done by placing two small sheets of lead across the opening from

[16] Davis and Mitchell, Phys. Rev. [2] 32, 331 (1928).

[17] Bearden, Phys. Rev. [2] 35, 1427 (1930).

[18] Gingrich, Phys. Rev. [2] 36, 1050 (1930).

[19] Jesse W. M. DuMond, Proc. Nat. Acad. 14, 875 (1928).

which the scattering body had previously been removed so as to leave a narrow slit at the center of the opening. Molybdenum radiation from an auxiliary tube passing through this slit diametrically across the cylindrical box fell on the quartz crystal. This latter was orientated and clamped so that the desired spectral region containing the K spectrum and extending from about 615 x.u. to 800 x.u. was reflected from the crystal. This entire region only subtended a breadth of about 0.4 mm in the scattering block.

The spectra were photographed at the end of a long lead camera with its small aperture as close as possible to the glass wall of the x-ray tube. Exposures of eight or ten hours sufficed for a beryllium scatterer, but an aluminum scatterer required exposures of fifty hours for a good spectrum. The spectra were taken on Eastman Duplitized film without any intensifying screen.

Microphotometer curves were taken across the spectrum in different regions of the height of the spectral lines and corresponding ordinates of these curves were averaged to reduce the accidental fluctuations of the film grain. The curves shown in Fig. 11 are the averages of five microphotometer curves in the case of the aluminum scatterer and three curves in the case of the beryllium scatterer. A linear relation was shown to hold between the deflections of the microphotometer and the x-ray intensities over the small range involved in these curves. This was done by a method described below in another section of this report.

The two small peaks, X_1, X_2 superposed on the long wave side of the broad modified line scattered by the beryllium are fluorescence lines of barium $K\alpha_1\alpha_2$ appearing in the second order. Barium fluoride and chloride is used as a flux in the preparation of metallic beryllium and the barium without doubt alloys to some extent with the beryllium. An extremely small quantity of barium is sufficient to produce strong fluorescence in comparison to the scattered spectrum because of the absorption of the barium atom following the Z^4 law.

The marked breadth of the modified line portrayed in these curves for both aluminum and beryllium scatterers is indisputable. The breadths at half maximum are of the order of 21 x.u. while the unmodified lines have a breadth of about
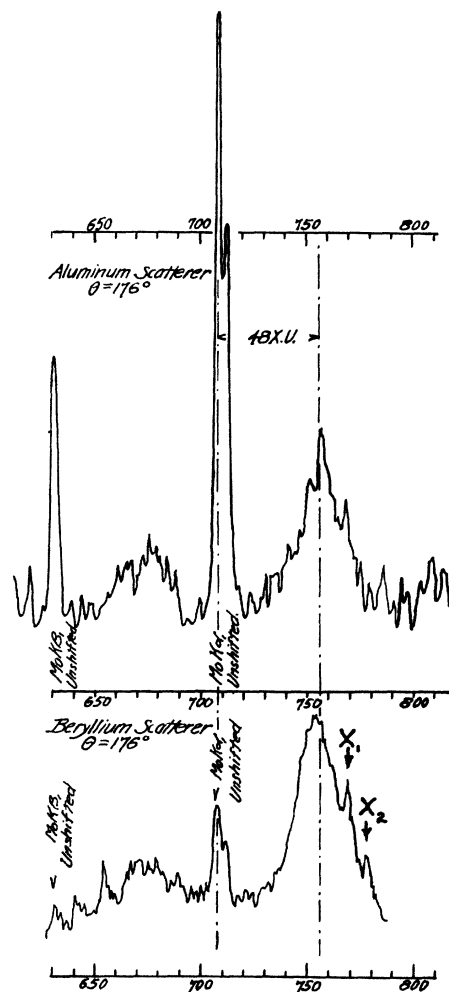

FIG. 11. Microphotometer curves of spectra of Mo K radiation scattered at 176° from aluminum and from beryllium scatterers.

1 x.u. The effect of inhomogeneity of the scattering angle would, in this case, increase the breadth less than 1 x.u.

9. Momenta of conduction electrons in beryllium

Further very interesting conclusions[20] were drawn from these spectral curves from metallic

[20] Jesse W. M. DuMond, Phys. Rev. [2] 33, 643 (1929).

scatterers as to the velocities possessed by the conduction electrons. These as derived from the curves proved to be in good agreement with the Fermi statistics. The curves proved the inapplicability of classical nondegenerate gas statistics by being strikingly discordant with the predictions of the latter. These conclusions however were based on the assumption that the author's interpretation of the breadth of the modified line as a Doppler effect of the initial velocities (or momenta) of the (bound and free) electrons in the scatterer was correct. The evidence for the correctness of this interpretation came later and is described at length in this article.

The evidence favorable to the applicability of the Fermi statistics and unfavorable to the applicability of the classical Boltzmann statistics in the case of conduction electrons is contained in the spectral curves of Fig. 12. They show for comparison the modified line structure or shape obtained for scattering of molybdenum $K\alpha_{1,2}$ radiation at large angles from beryllium (at the top) and the line structures theoretically predicted on several alternative assumptions as to the momenta of the electrons in the scatterer (below). In computing the theoretical curves the asymmetrical doublet character of the primary radiation was taken into account giving the curves a slight asymmetry. The ordinate scale of the theoretical curves was adjusted so as to normalize their areas to equality with the area under the experimental curve.

The velocities of conduction electrons satisfying the Fermi statistics are very much higher than one would expect to obtain if the Boltzmann statistics applied. The classical Boltzmann statistics require on the principle of equipartition of energy that the electrons shall have energies of the order $(3/2)KT$ corresponding to only about 0.04 volt. According to the Fermi statistics as applied to the "free" or conduction electrons in a metal by Sommerfeld[21] the application of Pauli's exclusion principle requires that only two electrons can occupy a phase cell of volume h^3. Thus some of the electrons are forced into high momentum states. In fact the density of electrons in momentum space is uniform out to a spherical boundary corresponding to a momentum of abso-

lute value P outside of which the electron density falls off to zero very abruptly. P, the maximum momentum of the degenerate electron gas, depends on the volume density, n, of the free electrons in the crystal lattice and is given by the formula

$$P = h(3n/8\pi)^{1/3}. \tag{29}$$

The temperature thus has very little to do with the electron velocities and indeed the only effect of increasing the temperature is to slightly reduce the abruptness of the boundary layer of radius P in the momentum space. Teṁperatures sufficient to appreciably destroy the degeneracy of the
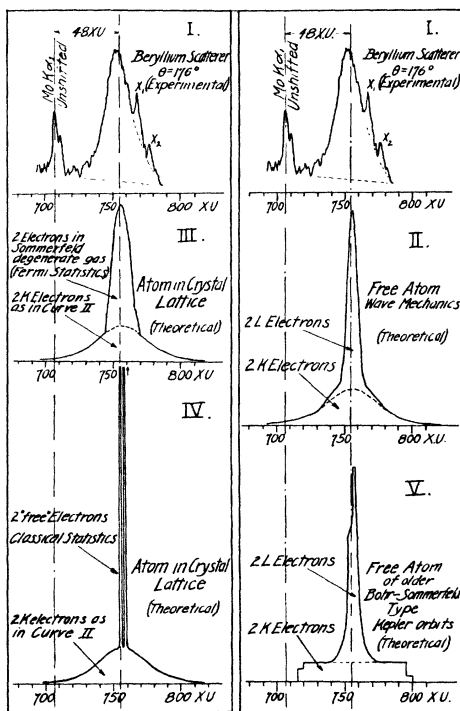

Fig. 12. Comparison of observed modified line structure (above) (Mo $K\alpha$ scattered from Be at 176°) with theoretical line structures computed on several alternative assumptions (below). The ordinate scales of the theoretical curves have been chosen so as to normalize the areas under the theoretical curves in each case to equality with the area under the experimental curve. For the case IV of two free electrons per atom obeying classical equipartition of thermal energy only, the line is so narrow that normalization of the area requires a height which cannot be conveniently represented on the diagram.

[21] A. Sommerfeld, Zeits. f. Physik. 47, 1 (1928).

electron gas in a metal far exceed the vaporizing temperature of the metal.

Assuming that the two L electrons of the beryllium atom are in the metal crystal lattice dissociated to form the free electron gas, we obtain an electron density of 2.5×10^{23} electrons per cm^3. The space charge of this enormous density is of course neutralized by the positive ions in the crystal lattice. The momentum P of the fastest of these free electrons should then, according to formula (29), be such as to correspond to a velocity of 2.24×10^8 cm/sec. or a kinetic energy of 14.2 volts.

The contribution of these Fermi-Sommerfeld electrons to the scattered spectral intensity distribution will be a broadened line, shown in Fig. 13, whose "shape" can be represented by an inverted parabola, as can be readily shown by
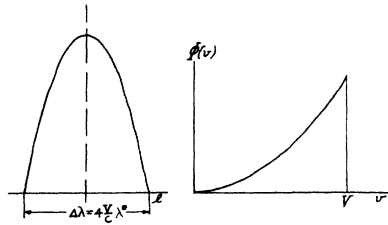

Fig. 13. On the right is shown curve of population of velocity (or momentum) states for "free" electrons in a conductor according to Sommerfeld's theory (assuming uniform potential throughout the interior of the crystal lattice). The distribution terminates abruptly at the momentum mV. On the left the resulting shifted line structure appears. This takes the form of an inverted parabola with a width at the base $=4\lambda^*V/c$.

application of formula (24). The width across the parabola at the base corresponds to the Doppler broadening of the fastest free electrons in the Fermi gas and applying the formula of Eq. (18) this width turns out to be for the case in question about 22 x.u. If the classical statistics be applied to the "free" electrons, it can be readily shown by the same methods that the shifted line would have the shape of a Gaussian error curve and a breadth at $1/e$ of its maximum intensity of 0.8 x.u. only. Thus the doublet structure of the primary radiation would be sharply reproduced in the modified radiation.

It is well worth while reminding the reader here that these computed spectral broadenings do

not correspond to the *energies* of the scattering electrons but to their *momenta*. An *energy* difference of 14 volts at wave-lengths of 700 x.u. corresponds to a very small wave-length change. We are here in the presence, not of a simple *spectral energy* shift, but a broadening produced by the *initial momenta* of the scattering electrons.

In computing the theoretical curves of line shape it is necessary to add to the contribution of the free or conduction electrons the contribution of the bound electrons to the modified scattering.

The modified wave-lengths for which the shift energy is too small to liberate a beryllium K electron occur so close to the unmodified wave-length that practically the entire curve for the K electrons is left intact. The faintness of the observed unmodified line is in agreement with this. Most of the observed unmodified line is doubtless caused by fluorescence of molybdenum sputtered or sublimed onto the scatterer from the focal spot of the tube.

The shape of the contribution to the modified line from the K electrons was computed by means of formula (24) with a quantum mechanical momentum distribution for the beryllium K shell derived in the manner outlined in the paper[3] by Podolsky and Pauling already mentioned.

Curve III, Fig. 12 then is the line shape to be expected from a solid beryllium scatterer in which two electrons per atom are dissociated to form the "free electron gas" and the two remaining K electrons are assumed to have their momentum distribution undisturbed by the proximity of neighboring atoms in the lattice. Curve IV is the line shape to be expected when two electrons per beryllium atom go to form a free electron gas satisfying the classical Boltzmann statistics, the K electrons being as before undisturbed. In order to normalize this latter curve to equal area with the experimental line structure the extreme narrowness of the two peaks requires a height far too great to represent to scale in the drawing. A very much smaller number of free electrons than two per atom could clearly be assumed and still give a computed curve in sharp discord with the observed curve which latter has not the slightest suggestion of a real double peak. *The evidence thus clearly contradicts the validity of the Boltzmann statistics for the free electrons in a metal and is in much better agreement with the Fermi statistics.*

The arbitrary division of electrons into two classes is a very rough approximation. Bloch has shown that all electrons have some chance of participating in conduction by passage *through* the potential barriers in the lattice. If this were taken into account the sharp breaks in curve III, Fig. 12, where the two separate structures join, would be smoothed out giving even better resemblance to the observed line structure.

Curve II, Fig. 12, is the line structure computed for a *free* scattering atom of beryllium, the two L electrons being assumed to have the momentum distribution required by quantum mechanics for an atom unperturbed by neighbors. It is not surprising that this should differ but little from curve III. The momenta of the outer electrons in the free atom are of the same order of magnitude as the momenta of the conduction electrons in the crystal lattice required by the Fermi statistics. Indeed the crystal lattice may be regarded as a large molecule in which the outer electron orbits of the individual atoms have coalesced to form long and complicated orbits common to the entire crystal.

Curve V, Fig. 12, is the line structure computed from the momentum distribution in a Bohr atom with point electrons executing classical orbital motions. The angularities of this distribution are quite evidently at variance with the experimental curve.

10. The multicrystal spectrograph

In order to test the validity of the foregoing interpretation of the modified line breadth and structure as a Doppler effect of electron momentum, it was necessary to study the behavior of the broadening as a function of primary wavelength and scattering angle. These two variables are the only ones involved in the effect which can be controlled. If the breadth could be shown to depend on these two variables in the way predicted by Eq. (18) this would give strong support for the Doppler-momentum interpretation.

To this end an especial spectrograph[22] was constructed to permit the study of scattered radiation with a wide variety of very sharply defined scattering angles. The instrument consists of fifty small cylindrical units, each a Zeeman type spectrograph in itself, placed vertically on

the arc of a horizontal circle of about a half-meter radius. Let us call this circle the "major circle" of the instrument. Each unit contains a brass wedge standing at about 0.1 mm distance from the cleavage face of a small slip of calcite. Figs. 14 and 15 show clearly the construction of these units. The units are orientated so that each
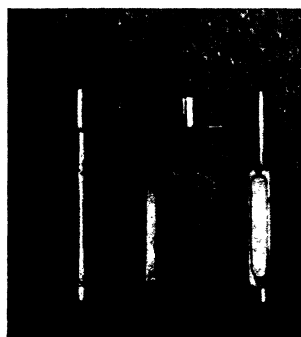

Fig. 14. Showing two of the fifty units of the multicrystal spectrograph, one of which is taken apart. The split sleeve is attached to the top of the curved bronze casting in which all the crystals stand by means of two small screws passing through the flat rectangular portion integral with the sleeve. A clamping screw passing horizontally through the casting compresses the sleeve on the shank of the crystal holder, thus clamping it.

calcite will reflect the $K\alpha$ doublet of molybdenum to exactly the same point on the photographic film. This film is rigidly maintained in a curved holder on the end of an adjustable swinging arm so that it coincides with an arc of the major circle on the side opposite the bank of crystals. If
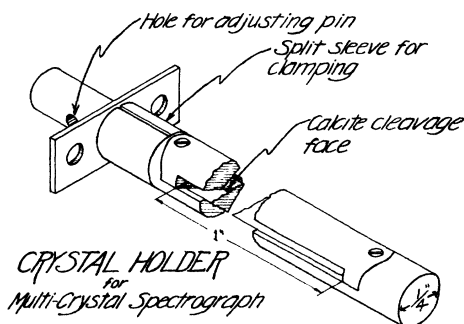

Fig. 15. Line drawing of crystal holder unit.

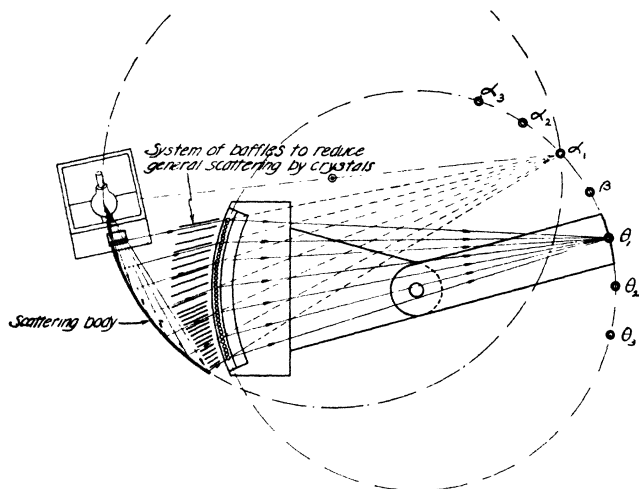[22] DuMond and Kirkpatrick, Rev. Sci. Inst. **1**, 88 (1930).

FIG. 16. Geometry of "focussing" and of homogeneity of scattering angle in the multicrystal spectrograph. θ_1, θ_2 and θ_3 show actual positions of K line of Mo in the first, second and third orders, respectively. The scattering body is here in position to give homogeneous scattering at 90° in the first order. β is the point where the reflecting planes of all the calcite crystals would converge if produced.

a given spectral line as reflected from all the crystals focusses or coincides at one point on the curved negative all other wave-lengths and orders will also focus at other points on the negative. In Fig. 16 a wave-length λ_1 is shown focussed from all fifty crystals at the point θ_1. The crystal reflecting planes if produced would all intersect at the point β on the major circle. The arc $\theta_1\beta$ is twice the Bragg angle for λ_1 reflected from calcite. The incoming radiation, if it were not reflected by the crystals to the point θ_1 would converge in a point α_1 also on the major circle. The arc $\alpha_1\beta$ is also twice the Bragg angle. We utilize the fact that the directions of incoming rays are concurrent at α_1. A second circle is described so as to pass through both the focal spot of the x-ray tube and the point α_1 corresponding to the mean wave-length of the modified line. The scattering body is shaped to coincide with this circle as shown in Fig. 16. Thus the scattering angle is very nearly homogeneous over all parts of the scatterer. Fig. 17 shows the positions of the spectrograph, the scatterer and the primary focal spot of the tube for three angles of scattering which were studied. The principle sources of inhomogeneity of scattering angle are the size of the

focal spot of the x-ray tube and the thickness of the scattering body. The use of fifty crystals instead of one permits the tube to be placed much farther away from the scatterer without necessitating unreasonable exposure times and thus permits a great reduction in the inhomogeneity of scattering angle from the two above-mentioned causes.

One of the most exacting and difficult requirements was to get good slips of calcite plane over their entire length. This requirement of planeness is necessary because the scattering body is an *extended* source of x-rays so that each point on the film receives x-rays reflected from all points over the entire length of the slit formed by the wedge and crystal. Thus a twisted crystal will give blurred diffuse spectral lines with an extended source whereas the same crystal would give sharp but inclined or bent lines with a point source. Our first care was therefore to test the planeness of our crystals by means of primary radiation from an x-ray tube placed a short distance in front of the spectrograph. As the tube had a small focal spot and was much nearer the crystal than was the negative, only a small portion of the length of the crystal was used in form-
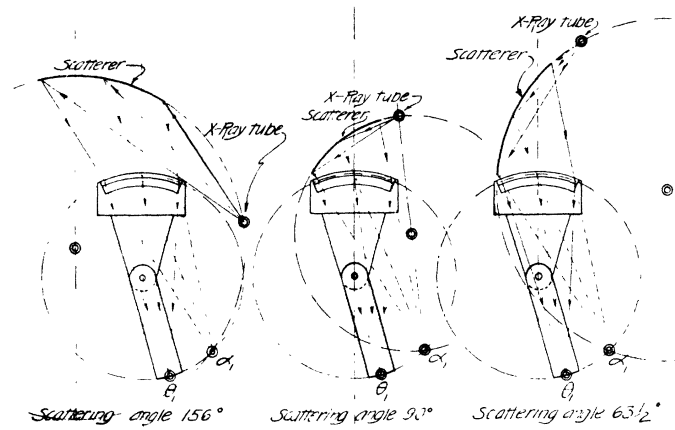
FIG. 17. Geometrical dispositions of x-ray tube scatterer and spectrograph for three different scattering angles.

ing the entire length of the lines on the negative. By moving the x-ray tube vertically parallel to the wedge of the Zeeman spectrograph any region in the height of the crystal could be used to reflect spectral lines to the negative. By this means we compared for each and every crystal the position of lines reflected from the midpoint of the crystal with their positions as reflected from four other points along its height. Good exposures for these tests with primary radiation could be obtained in 45 seconds. Shields were used in front of the negative so that the lines from the midpoint of the crystal appeared in the middle of the film while the lines from the four other points were screened off in this region and appeared at the edges of the film. There were thus four double exposures to test the planeness of each crystal, the film being displaced slightly between each pair of exposures. Generally an extra pair of exposures was taken comparing one extreme end of the crystal with the other end. Since these films look almost exactly like the orientation exposures shown in Fig. 18, they are not reproduced here. Crystals that failed to reflect lines to the same point by less than half the breadth of a line (or about half an X-unit on our spectrograms) over the entire length of crystal were discarded. The

backs of the crystals had to be ground to fit into their holders before such tests had any significance and on account of the numerous discards this constituted one of the most tedious features of the experiment. We take a pardonable pride therefore in calling attention to the sharpness of the unshifted lines we have obtained. This sharpness bears witness to the planeness and perfection of each and every one of the fifty crystals used as

5. 6 12. 19

FIG. 18. Typical film obtained in orientating crystals. The adjustment of number 6 is acceptable. In each of these four cases the pair of lines at the edge is formed by an exposure with the reference crystal (the center being blocked off with a shield) while the pair of lines in the center is formed by an exposure with the crystal under test (the edges being blocked off). As a precaution against confusion a short portion is also blocked off in the center on alternate exposures of crystals under test. The pair of lines is the $K\alpha$ doublet of molybdenum. The exposures made for testing individual crystals for their "planeness" were entirely similar to these save that in them the lines reflected from different regions of the same crystal were compared.

well as to the accuracy with which they are focussed.

The focussing of the crystals was accomplished photographically. After fifty good crystals mounted in the cylindrical Zeeman units in the spectrograph had been obtained, one of these near the center was permanently clamped in a predetermined orientation so as to reflect the Mo $K\alpha$ lines in a convenient position on the films. This was called the reference crystal. The other forty-nine units were first roughly orientated by means of a fluoroscopic screen so as to reflect their lines to the same point on the film within a few millimeters. Direct radiation was used, the Mo tube being mounted in a lead box in front of the spectrograph on a large wooden sector turning on a pin directly under the point α_1. Divisions marked on the circular edge of this sector made it possible at a moment's notice to align the tube with any desired crystal. A lead shield was used to isolate all but the crystal under test. The fine adjustment of the crystals consisted in taking a photograph of the $K\alpha$ lines with the reference crystal and then without disturbing the negative taking the $K\alpha$ lines with the crystal to be adjusted. Again shields were used in front of the negative so that the reference lines appeared in the middle of the height of the negative while the lines from the crystal under test appeared just above and below. When the focussing of a crystal was acceptable its lines joined those of the reference crystal forming continuous lines across the negative with no perceptible break or jog at the two junction points. Forty-five second exposures were used. A complete set of forty-nine such pairs of exposures was made, testing the state of adjustment of all crystals against the reference crystal. These exposures appearing on ten pieces of film were all developed, fixed, and dried at one time in an especially designed holder, thus economizing enormously on the time in comparison to what would be required for separate development. A sample of such a film is shown in Fig. 18. Each crystal was then turned through the angle demanded by the error in adjustment indicated in the photographs. This could be done with considerable accuracy, thanks to a small gilded plane mirror permanently mounted on top of each crystal holder. The reflection of a scale three meters distant from the mirror was ob-

served with a telescope as a means of measuring the angles through which the crystals must be turned to correct the error indicated on the photographs. Each crystal was provided with a small steel lever at the end of which two adjusting screws permitted us to make the fine adjustment of orientation and clamp the crystal in its new position. After making the indicated orientation adjustments, a second set of forty-nine pairs of comparison photographs was taken. A few of the crystals were found to be in acceptable register with respect to the reference lines. These were eliminated from the remainder of the work by dropping small brass covers over their adjusting screws. The cycle was then repeated and each time more and more crystals came into acceptable adjustment until finally all had been satisfactorily adjusted. The author here wishes to express his unbounded appreciation of the excellent and painstaking work of his collaborator, Dr. H. A. Kirkpatrick, in making these difficult adjustments.

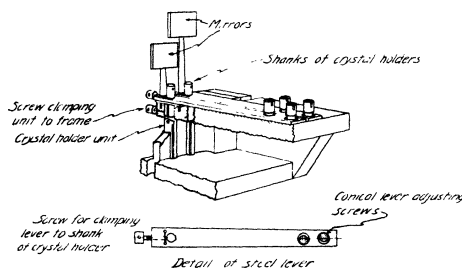Fig. 19 shows in detail the construction of the crystal unit adjusting levers and the holder in

FIG. 19. Showing crystal holder units in place in the bronze casting of the multicrystal spectrograph. The casting is shown cut away so that only two crystal holders at the extreme end of the assembly are visible. In the detail view of the lever for the fine adjustment of the orientation of the crystals the screw clamping this lever to the shank of the crystal holder operates by slightly deforming the thin side of the hole surrounding the shank. The opposite side of the hole is relieved with a rectangular keyway so that the lever bears on the cylindrical shank at three distinct points. The mirror supports are soldered to the rear end of the levers.

which the crystal units stood. The lever can be clamped at one end to the projecting shank of the crystal holder without marring the shank. The other end of the lever is given a slight sidewise motion to right or left by two conical-headed

screws pressing on opposite sides of two oversize conical holes in the end of the lever. The latitude of motion is considerably restricted by the neighboring levers, but when more rotation was required than could be obtained in the travel of the lever the shank of the crystal holder could be clamped to its supporting frame and the lever unclamped from the shank and returned to the opposite end of its travel. The clamping of the crystal holder to the supporting frame was accomplished by a screw through the frame which pressed on the split sleeve (see Fig. 15) surrounding the crystal holder shank. The frame supporting the crystal holders was a curved bronze casting whose cross section was the shape of a capital letter L. The fifty crystal holders fitted accurately in fifty holes bored in this bronze casting as close together as consistent with mechanical strength and accurately located on the major circle of the

instrument. The curved casting had two channels milled out on either side to a depth such that the fifty holes each open into the channels so as to form two elongated rectangular windows on diametrically opposite sides of each hole. The x-rays pass through these windows. The "hour glass" cross section of the bronze casting which remains between two adjacent holes provides an arc of contact of nearly 90° on two opposite sides of each crystal holder. This is amply sufficient to prevent x-radiation from leaking between the crystal holders.

The small gilded mirrors stand staggered in two rows on the ends of supports fastened to the steel levers. Alternate crystals have their mirrors in the upper and lower rows so as to permit the largest possible dimensions for the mirrors in the available space.

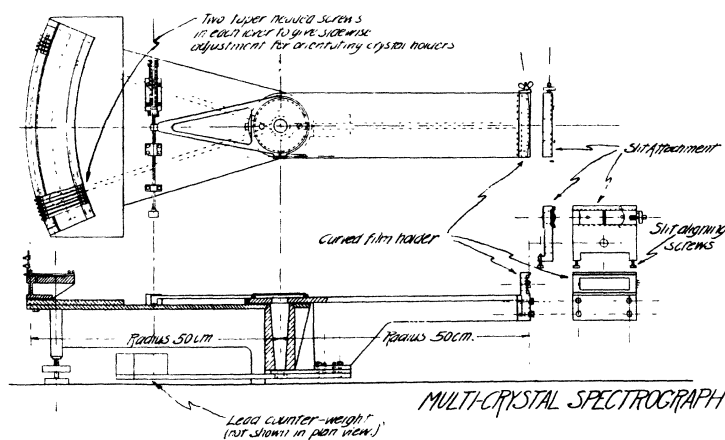Fig. 20 is a general plan and elevation of the

FIG. 20. Plan and elevation of multicrystal spectrograph.

instrument and Fig. 21 is a photograph with the cover of the lead enclosing box removed to show the general arrangement.

The curved scattering body, the focal spot of the x-ray tube and the point α of the spectrograph are made to lie on the same circular arc by means of a plumb-line suspended from the end of a swinging radius arm. The x-ray focal spot is aligned with this plumb-line by sighting from two directions with auxiliary plumb-lines. By measuring the angle through which this radius rod

must turn in passing from α to the x-ray focal spot the scattering angle was measured with more than adequate accuracy. Fig. 22 is a general view of the set-up in which this radius arm is clearly visible.

11. Cause and elimination of heavy background

It has been noted by many observers that the background intensity relative to the line intensity in the spectra of scattered radiation is much stronger than in spectra of primary radiation. We

FIG. 21. General view of multicrystal spectrograph with cover of lead enclosing box removed. The baffles for reducing the fogging caused by diffuse scattering can be clearly seen as can also the curved graphite scattering body in the foreground.

believe that the suppression of this background by the method about to be described proves that its principal cause is nonselective scattering at the crystals and wedges. General, amorphous or nonselective scattering by a crystal is the result of scattering of the Compton type. Such scattering is incoherent and hence nonselective as to wave-lengths. It is also nonspecular in that the condition of equality of incidence and reflection angles does not hold. This means that a given point on the negative can receive radiation of all wave-lengths from all parts of the scattering body by this type of scattering. This same point on the negative can, by spectrally selective Bragg reflection, only receive one wave-length scattered from one very small part of the scattering body. Though the modified scattering at the crystals and wedges may be small, it is greatly favored by the fact that it is integrated over a wide range of continuous spectrum and over a broad solid

Fig. 22. General view of experimental set-up. Note the radius arm and plumb-line for locating the focal spot of the tube and the position of the scatterer. This plumb-line is aligned with the focal spot by sighting with auxiliary plumb-lines through the aperture in the tube housing at the left and through the x-ray port. The scattering angle is determined accurately by measuring the angle through which this arm rotates in passing from the focal spot to the point α_1 (Fig. 16), the angle of rotation being measured on the disk clearly visible in this figure.

angle as large as the scatterer can subtend. With these considerations in mind we tried the effect of introducing a set of baffle plates in front of the spectrograph in such a way as to greatly limit the solid angle of radiation "seen" by the crystal and wedge. The baffles leave plenty of room for the formation of the entire shifted and unshifted K spectrum, however, which only requires a range of about three degrees. The baffles are also so situated as to cut off the "straight through" radiation that could otherwise pass between wedge and crystal without reflection. These baffles can be plainly seen in Fig. 21 and they are also shown in Fig. 16. Different sets of baffles were constructed for different scattering angles and primary wavelengths.

12. Increase of modified line breadth with scattering angle experimentally verified

Fig. 23 shows three spectra of molybdenum K radiation scattered from graphite at three very homogeneous scattering angles, the scattering angle and inhomogeneity being indicated in each case on the figure. The increase in modified line breadth with increasing scattering angle predicted by the theory of initial electron momenta is clearly evident. A few of the microphotometer curves taken from these negatives are shown in Fig. 24, and in Fig. 25 the theoretical curve of

dependence of breadth on scattering angle is plotted for comparison with the points corresponding to observed breadths. The ordinate scale is adjusted to make the grand average of the points for the largest scattering angle coincide with the curve. The points for other scattering angles then fall where they will. We thus have a test not of the absolute value of the breadth but of its variation with scattering angle. The agreement is seen to be as good as the reproducibility of the breadth measurements. Attention is called to the fact that the average breadths of shifted α are systematically higher than the average breadths of shifted β in accord with the theory and with the experimental results about to be described for the dependence of breadth on primary wave-length.

Methods of correcting for the doublet character of the shifted line will be described in a later section of this article.

13. Increase of modified line breadth with increasing wave-length experimentally verified

Fig. 26 is a reproduction of three negatives of molybdenum, silver and tungsten K radiation scattered from graphite at very nearly the same homogeneous scattering angle. The theoretically predicted increase in shifted line breadth with increase in primary wave-length is evident. For tungsten radiation scattered at large angles from graphite we did not expect to obtain any unmodified lines at all and, as can readily be seen, none appeared. Ordinarily the unmodified lines serve admirably as fiducial lines to establish the wave-length scale. In the case of tungsten radiation reference lines were established on the edges of the film by making an auxiliary exposure with primary tungsten radiation from a Coolidge tube placed in front of the spectrograph in the position of the scatterer which had been removed for this purpose. A lead shield in front of the negative during this exposure permitted the lines to appear only at the edges to avoid all risk of fogging or falsifying the valuable 1020 hour exposure with scattered radiation. The Coolidge tube in the auxiliary exposure was slowly moved across the front of the spectrograph so that all the crystals were brought into play, thus giving a good *average* position to the fiducial lines instead of their position for one crystal only.
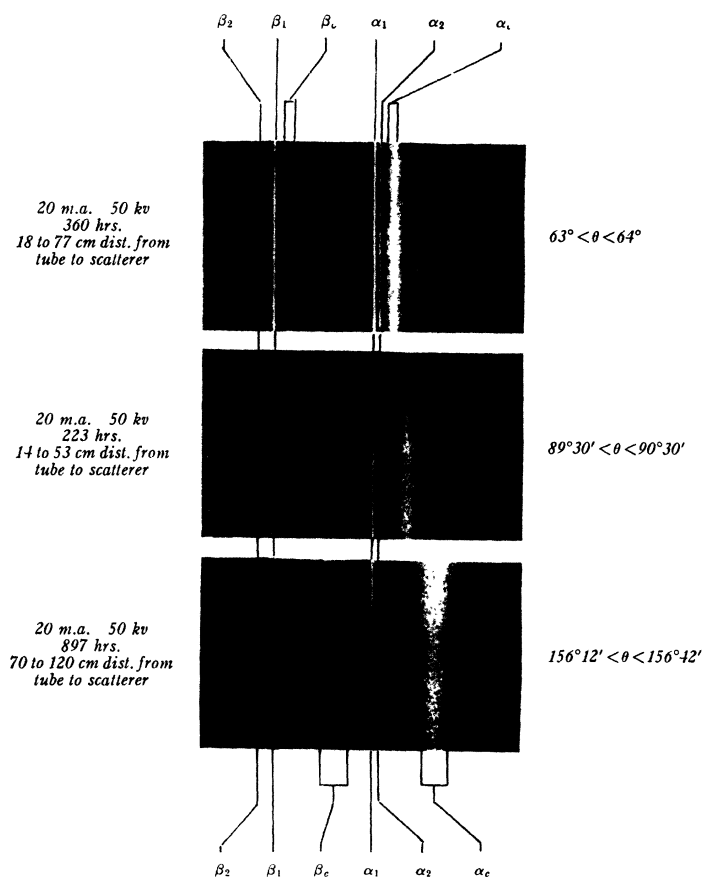
Fig. 23. Spectra of Mo K radiation scattered at three very homogeneous scattering angles from graphite, taken with the multicrystal spectrograph. Note sharpness of unshifted lines and increasing breadth of shifted lines as scattering angle increases.

Fig. 27 shows three typical microphotometer curves taken from these negatives and in Fig. 28 the observed breadths at half maximum are plotted for comparison against the curve of dependence of breadth on primary wave-length required by the theory. Here again the ordinate scale was adjusted so that the largest average breadth fitted the theoretical curve, the other points for shorter primary wave-lengths being allowed to fall where they would so as to furnish a test of the functional dependence.

14. Critical discussion of these results

The success of the author's theory in predicting these two new physical effects would seem to be the strongest evidence for the correctness of the ideas underlying it. We see that the atom does in fact behave toward radiation just as though it contained electron momenta capable of impressing a Doppler broadening on an initially sharp x-ray line. We shall see below furthermore that the momenta deduced from a study of the spectral distribution of the broadened line is in con-
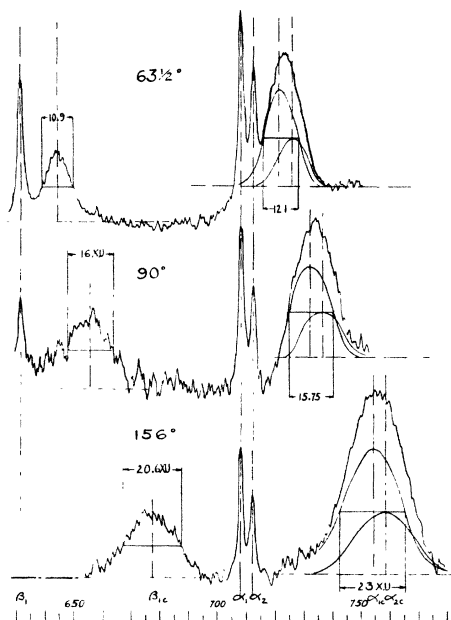
FIG. 24. Microphotometer curves of the spectra shown in Fig. 23. Five such curves for each scattering angle were obtained by running the microphotometer slit across the lines in different regions of their height. The three curves here shown are fairly typical of the entire set.

sistent agreement with the momenta predicted by quantum mechanics.

The author purposely uses this behavioristic terminology because it is the only one which our present knowledge justifies. If the quantum mechanics and the uncertainty principle are correct, nothing can be said about the instantaneous value of the momentum of an electron in an atom as the result of a physical measurement. The quantum mechanics permits us to predict only the probability distribution of the results of a large number of observations over an extended time. This, of course, is precisely what is observed in the broadened modified line. It is very interesting to see that a simple picture of the mechanism of scattering such as the author has presented leads so satisfactorily to results in accord with both the facts and the quantum theory.

The reality of the observed effects can scarcely be questioned from the experimental side. The

reality of the breadth has been checked by the author in collaboration with A. Hoyt by the independent method of the double crystal spectrometer.[23] The possibility of broadening by multiple scattering has been investigated both theoretically[24] and experimentally[25] and eliminated completely. *Recently P. A. Ross at Stanford has succeeded in getting excellent spectral curves of the modified line with his double crystal spectrometer which not only are in complete accord with the breadths reported here but which also reveal the variation in breadth with scattering angle in accord with the author's theory and observations.*

D. MOMENTUM DISTRIBUTION IN CARBON

15. Photographic and microphotometric calibration

It is necessary first to establish the relationship between the ordinates of the microphotometer curves and the corresponding scale of x-ray intensities. This was done by an independent cali-
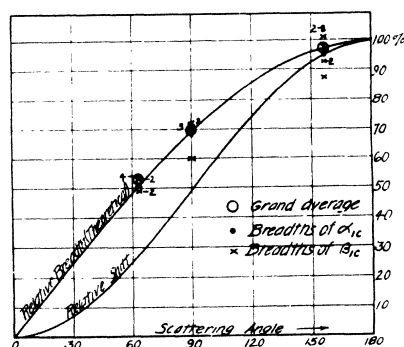

FIG. 25. Measured breadth of shifted lines compared with theoretical prediction of functional dependence of breadth on scattering angle. The theoretical dependence is derived on the assumption that the breadth is caused by the initial momenta of the scattering electrons and the experimental points are seen to support this theory. The ordinate scale of the curve has been adjusted to pass through the observed grand average breadth at 156°, the other points falling where they will. This is therefore a test of the *variation* in breadth with scattering angle rather than a test of the absolute value of the breadth. Note that the breadths of shifted β are systematically lower than the breadths of shifted α in accord with the predicted dependence of breadth on primary wave-length.

[23] DuMond and Hoyt, Phys. Rev. [2] **37**, 1443 (1931).

[24] Jesse W. M. DuMond, Phys. Rev. [2] **36**, 1685 (1930).

[25] Jesse W. M. DuMond and Harry A. Kirkpatrick, Phys. Rev. [2] **37**, 159 (1931), (see the last paragraph).

20 m.a. 50 kv
897 hrs.

*Molybdenum K
primary scattered at
156°27'±15'*

13 m.a. 50 kv
900 hrs.

*Silver K primary
scattered at
155°21'±15'*

10 m.a. 118 kv
Intensifying screen
1020 hrs.

*Tungsten K primary
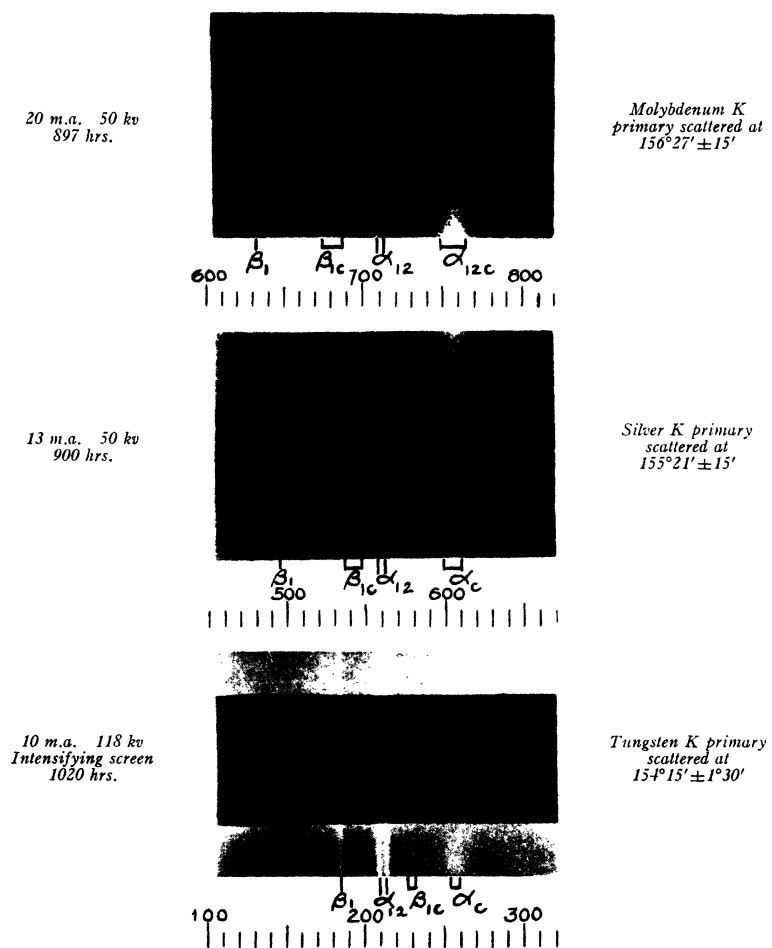scattered at
154°15'±1°30'*

FIG. 26. Three spectra of *K* radiation scattered by graphite at about 156°. The dispersion in wave-length units is the same on all three exposures as can be seen by observing that the Compton shift for the *Kα* lines is the same in all three cases. (At such a large scattering angle the slight variation in scattering angle between the three cases produces no detectable difference in shift.) Note the very evident diminution in the breadth of the shifted line measured in wave-length units as the wave-length diminishes. The unshifted lines are completely absent in the case of tungsten radiation scattered from graphite. The reference lines on the edges of this film made by an auxiliary exposure with direct tungsten radiation are slightly broadened by over-exposure in combination with the effect of an intensifying screen. This is the only film on which an intensifying screen was used.
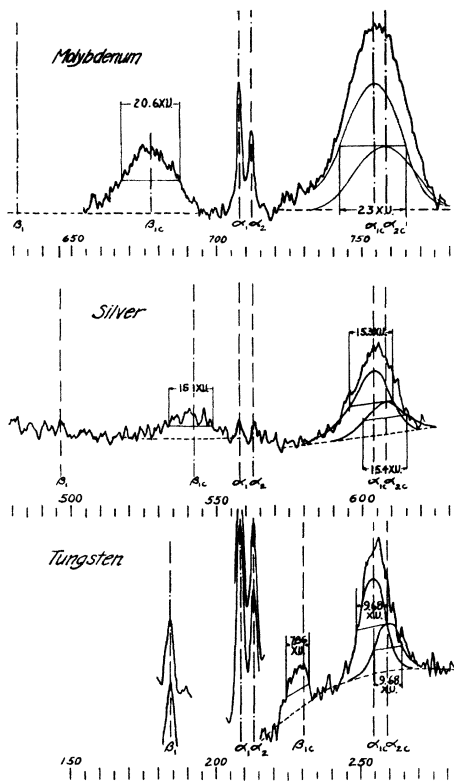
FIG. 27. Three typical microphotometer curves taken from the spectra of Fig. 26. A number of such curves were run on each negative in different regions of the height of the spectral lines. In the case of the tungsten spectrum the position of the reference lines had to be recorded by making two separate runs across the two edges of the film. This could be easily accomplished as the table carrying the negative on the microphotometer can be shifted laterally accurately normal to its direction of travel.

bration experiment. A monochromatic x-ray line was isolated by means of a crystal spectrometer. An exposure disk shown in Fig. 29 was caused to rotate so as to expose a photographic film to various portions of this line for varying intervals of time. The disk was very carefully cut and calibrated so as to give the exposure times in steps of one-tenth the total exposure; the first step one-tenth of total exposure, the second two-tenths, etc. The film was slowly translated with a uniform oscillating motion at right angles to the length of the spectral line by means of a carefully cut cam

so as to spread the stepped exposure into a stepped band of convenient width for use in the microphotometer. A number of these stepped calibration bands were made up with varying degrees of blackening. Microphotometer curves of a given modified line distribution were then made and immediately afterward, without changing any adjustments on the microphotometer, a stepped curve was run on the same recording plate with one of the stepped calibration negatives chosen so that its range of blackening and microphotometer deflection would embrace the range of the modified line spectrum negative. Considerable study was given to the effect of development time, the variation in different samples of calibration film, the variation in the original intensity along the length of the spectrum line, the possible effect of the speed of the serrated disk (intermittency effect), and the effect of different initial x-ray intensities and exposure times. Fortunately, however, these sources of error can all be neglected because the results of this calibration work showed conclusively that in our spectral photographs the range of blackening in the modified line embraced such a
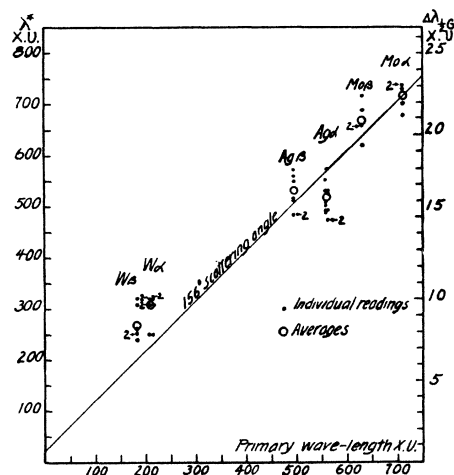

FIG. 28. Comparison of observed breadths of modified lines for different primary wave-lengths with the theoretically predicted functional dependence of breadth on primary wave-length. The ordinate scale on the left is λ^* in x.u. The ordinate scale on the right is the breadth in x-units of the modified line at half maximum value, adjusted to fit the theoretical curve at one point only, namely the observed breadth of shifted Mo $K\alpha_{1, 2}$.
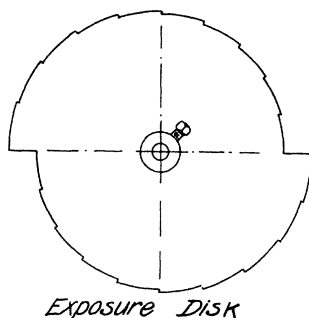
Exposure Disk

FIG. 29. Serrated disk used for exposing different portions of a monochromatic x-ray line for intervals of time varying in one-tenth steps of the total exposure. The disk is disposed so that the x-ray line stands radially across the periphery. The photographic film immediately behind the disk is given an oscillating motion of uniform translation normal to the x-ray line so as to spread the exposure into a uniform stepped band.

small part of the blackening curve that the relationship was sensibly linear over the entire region of interest. Fig. 30 is a sample curve made with the exposure disk relating microphotometer deflections as ordinates to exposure as abscissae. The two horizontal lines correspond to the highest and lowest deflection of the microphotometer in the case of a sample spectral curve of the modified line. The vertical deviation of the secant line drawn through the intersections of the horizontal lines with the curve gives an idea of the very small relative correction required in the ordinates of the microphotometer curves. This correction has therefore been considered insignificant and has not been applied.

16. Analytical separation of superposed shifted component lines

Modified $K\alpha_1$ and modified $K\alpha_2$ are always confounded into one band because the breadth of these two modified lines always greatly exceeds the 4 x.u. separation between them. As this is the most intense modified line available, use must be made of it in spite of this difficulty. Fortunately, enough information is available to permit an analytical determination of the line shape for one component line alone, given the curve of the two superposed lines, thanks to the fact that the separation of the components and their relative intensity is accurately known.

The simple method first used is made clear in Fig. 31. Let $F(x)$ be the function representing the observed line structure, and $f(x)$ the contribution to $F(x)$ made by the α_1 line. Then the contribution made by the α_2 line will evidently be $kf(x-\delta)$ where $k=\frac{1}{2}$ and $\delta=4$ x.u., the known intensity ratio and wave-length separation of α_1 and α_2. We have then

$$F(x) = f(x) + \tfrac{1}{2}f(x-\delta), \tag{30}$$

where $F(x)$ is experimentally given and $f(x)$ is to be found. It is easy to show by substitution from the last equation that

$$f(x) = F(x) - \tfrac{1}{2}F(x-\delta) + \tfrac{1}{4}F(x-2\delta)\cdots \tag{31}$$

for on substituting the values of $F(x)$, $F(x-\delta)$, etc., in the right-hand member all terms cancel in pairs save the first term $f(x)$ and the last term
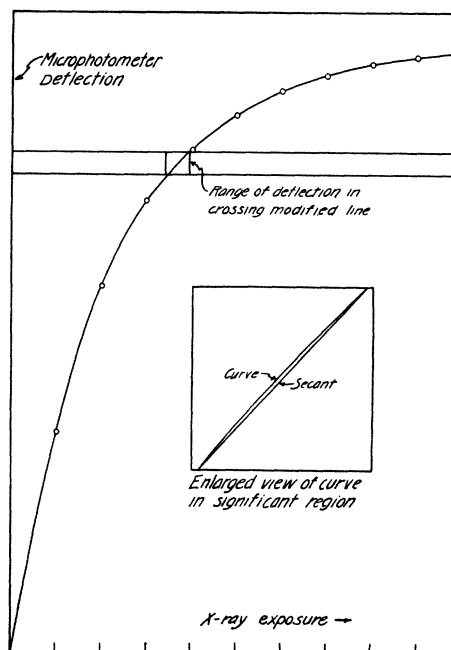

FIG. 30. The curve is a plot of microphotometer deflections against x-ray exposures with a monochromatic line used to blacken the calibration film. The amplitude of the microphotometer deflections in exploring a typical spectral curve of the modified line is also plotted. The departure of the curve from its secant over this small region is seen to be very small.

of the form $\pm(1/2^n)f(x-n\delta)$. This last term can be made as small as desired because the line structure falls off rapidly to zero as we recede from the maximum. In practice the decomposition is rapidly effected as follows. Referring to Fig. 31, equally spaced vertical ordinates are erected with the spacing, δ, corresponding to
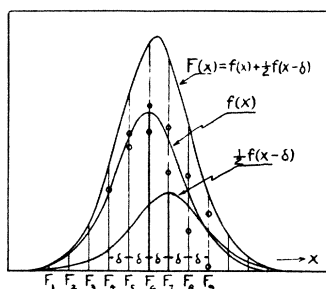

FIG. 31. Illustrating one method of decomposing line structure curves from the $K\alpha$ doublet.

the exact separation of the $\alpha_1\alpha_2$ doublet. The value of the ordinate F_4 say is corrected by subtracting from it half the value of F_3, its first neighbor to the left. Then adding a quarter of F_2, subtracting an eighth of F_1, etc., until the correction becomes negligible. The alternating nature of the series makes it easy to be sure when this point is reached. It is easy to check the work by adding the two component curves and comparing their sum with the original curve.

Now this method of procedure can be generalized to permit the separation of any number of functions of the same shape but with specified intensity ratios and relative displacements. It is proved in the calculus of finite differences that an operator Δ defined to have the property of changing $f(x)$ into $f(x+\delta)$ will obey the laws of algebra. It follows that the binomial or polynomial theorem can be applied to a polynomial in Δ. The general case for any number of superposed spectral lines of the same shape can be expressed as

$$F(x)=\sum_{i=1}^{n}k_if(x+\delta_i)\qquad(32)$$

where f is to be found, given F. This can be symbolically written

$$F(x)=\sum_{i=1}^{n}k_i\Delta_i f(x)=f(x)\sum_{i=1}^{n}k_i\Delta_i.\qquad(33)$$

Solving this equation for $f(x)$ we have

$$f(x)=F(x)\left(\sum_{i=1}^{n}k_i\Delta_i\right)^{-1}.\qquad(34)$$

The polynomial in $k_i\Delta_i$ can then be expanded by the polynomial theorem. The interpretation of $\Delta_i{}^n$ is of course $F(x+n\delta_i)$.

We shall make use of an interesting special case of this generalization. Suppose we have given a line structure function $F(x)$ which is the sum of two *identical* line structures separated by a known distance $2\delta'$

$$F(x)=f(x+\delta')+f(x-\delta').\qquad(35)$$

Then the function $f(x)$ can be found by the formula

$$f(x)=F(x+\delta')-F(x+3\delta')+F(x-5\delta')\cdots.\qquad(36)$$

As before this can be readily checked by a direct substitution.

We have applied this to the analysis of modified line structures as follows: Referring to Fig. 32, curve 1 is the modified line structure obtained
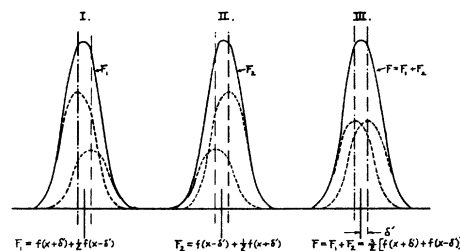

FIG. 32. Illustrating the symmetrical method of decomposing line structure curves into their two alpha-components.

by averaging a number of microphotometer curves and subtracting from them a smooth background curve (generally very nearly a straight line) obtained by interpolating from the observed background on either side of the modified line. (This estimation of the background is admittedly an uncertain process and one of the chief causes of uncertainty in the results.) Curve

2 is obtained by plotting curve 1 *reversed* so as to make the position of shifted α_1 fall on the position of shifted α_2 and *vice versa*. The positions of shifted α_1 and shifted α_2 can be accurately located since the scattering angle is known accurately. Curve 3 is the sum of 1 and 2. It is clear that the curve now consists of two *equal* components of the desired structure separated by the known wave-length separation of the alpha-doublet and we have the added advantage of averaging out accidental fluctuations which disagree on the two sides of the line. It is clear that this artifice for rendering the structure symmetrical is justified for the interpretative purpose to which this study of line structure is to be applied for, if the structure were appreciably asymmetrical, our theory would interpret this as a drift of a prodigious number of electrons in one direction through the scatterer corresponding to an electrical current of fantastic proportions. We have now only to apply the formula (36) to curve 3 to obtain the corrected modified line structure.

17. Experimental and theoretical momentum distributions

We now apply formula (25) to the corrected line structure to obtain the momentum distribution which represents the probability of observing an electron with linear momentum of absolute value P in the range dP. The process consists simply in taking the product of the slope of the line structure curve at each point by the corresponding abscissa and plotting this as an ordinate at that abscissa. The abscissae l of the line structure curve are in wave-lengths but these are easily transformed to a scale of $\beta = v/c$ by means of the formula (14) which is with sufficient accuracy for the values of β involved simply $l = 2\beta\lambda^*$, λ^* being given by formula (15). The momentum P is $m\beta c$.

In Fig. 33, curve 1 is a half profile of the modified line after applying all of the corrections here described. This curve which is the best one so far obtained represents the modified line shape for molybdenum radiation scattered at 156° by a graphite scatterer. Curve 2, Fig. 33, is the momentum distribution derived from curve 1. We have taken the liberty of "smoothing" curve 1 as can be seen by the discrepancies between the points and the curve. The roughly periodic fluc-
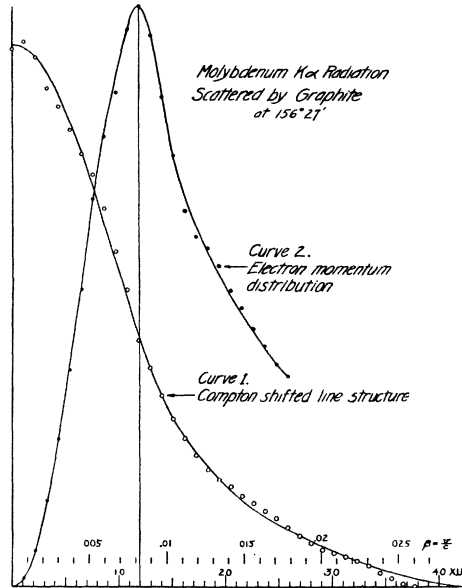

Fig. 33. Half profile of a typical modified line structure after application of all corrections and the resulting derived electron momentum distribution. The abscissae for the line structure are in x.u. and for the momentum distribution in $\beta = v/c$. The momentum is $p = m\beta c$.

tuation of the points above and below the smooth curve is perhaps introduced by the process of decomposing the doublet line structure into its components. If our interpretation of the modified line structure is correct, curve 1 must decrease monotonically as we recede from the peak for a reversal in slope would mean a *negative* probability. Small reversals of slope indicated by the points are simply the residual effects of film grain in the original negative.

In Fig. 34 a theoretical distribution of momentum P in the carbon atom has been plotted. This was computed by means of the Podolsky-Pauling formula given in Eq. (27). The formula was applied to carbon by assigning an effective atomic number $Z = 5.7$ for the K electrons and $Z = 3.25$ for the L electrons. These values were chosen as suggested by Slater[26] without any attempt to fit our observations. The three component curves correspond to a circular K orbit, a circular L

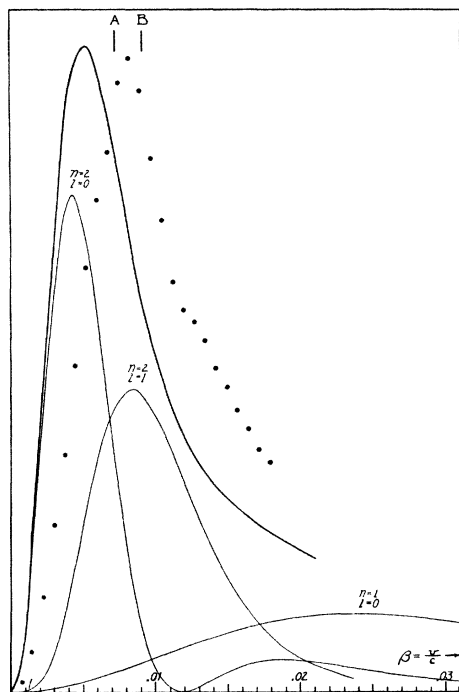---

[26] Slater, Phys. Rev. [2] **36**, 57 (1930).

FIG. 34. Comparison of theoretically computed momentum distribution in a free carbon atom with experimental result of Fig. 33 obtained for graphite.

orbit and an elliptical L orbit of the classical Bohr theory. It is interesting to note the two maxima in the curve corresponding to the elliptical orbit. The high maximum of this pair is the analogue of the minimum momentum occurring at aphelion and the low maximum that of the maximum momentum at perihelion.

The experimental momentum distribution is seen to be strikingly similar in *shape* to the theoretical curve. The position of its maximum occurs at somewhat higher momenta than the maximum of the total theoretical curve *but agrees well with the most probable momentum for the "circular" L orbit* (quantum numbers $n=2, l=1$).

Now it must be remembered that our theoretical curve is computed for an isolated carbon atom while our experiment is performed on a graphite scatterer. The effect of bringing carbon atoms together to form a solid body is precisely to disturb the outer orbits and in general to require higher electron momenta of them. What happens to the outer electrons in graphite is problematical but it seems plausible to suppose that the orbit which will suffer the greatest modification will be the "elliptical" one and that this modification will be in the direction of higher momenta. If we compute the momentum distribution replacing the two L electrons in the elliptical orbit with two electrons in a Fermi gas the limiting velocity of this gas occurs at the value $\beta = 0.0075$. This would give a very sharp maximum at this point whose position agrees much better with the position of the maximum of the curve derived from experiment.

However, the Fermi-Sommerfeld gas is only a rough approximation to'the truth in a crystal lattice and the true momentum distribution of the disturbed electron orbits should merge imperceptibly into the momentum distribution of the entire atom. Instead of the sharp peak at $\beta = 0.0075$, one should expect a softened maximum at this position of much the same type as the curve for the quantum numbers $n=2, l=1$.

At A and B in Fig. 34 are shown the positions of the peak of the curve computed for a Fermi-Sommerfeld electron "gas." A is the position if the gas consists of *two* electrons per atom and B is the position if the gas consists of four electrons per atom. The four L electrons are by far the most likely to suffer modification in the solid state. We believe therefore that the observed momentum distribution (represented by the dots in Fig. 34) is entirely consistent with theoretical expectations.
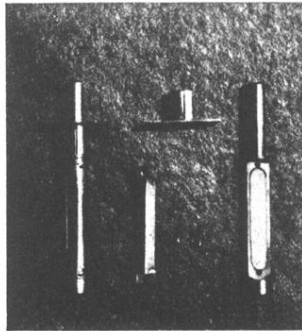
FIG. 14. Showing two of the fifty units of the multicrystal spectrograph, one of which is taken apart. The split sleeve is attached to the top of the curved bronze casting in which all the crystals stand by means of two small screws passing through the flat rectangular portion integral with the sleeve. A clamping screw passing horizontally through the casting compresses the sleeve on the shank of the crystal holder, thus clamping it.

5.   6   12. 19

FIG. 18. Typical film obtained in orientating crystals. The adjustment of number 6 is acceptable. In each of these four cases the pair of lines at the edge is formed by an exposure with the reference crystal (the center being blocked off with a shield) while the pair of lines in the center is formed by an exposure with the crystal under test (the edges being blocked off). As a precaution against confusion a short portion is also blocked off in the center on alternate exposures of crystals under test. The pair of lines is the $K\alpha$ doublet of molybdenum. The exposures made for testing individual crystals for their "planeness" were entirely similar to these save that in them the lines reflected from different regions of the same crystal were compared.

FIG. 21. General view of multicrystal spectrograph with cover of lead enclosing box removed. The baffles for reducing the fogging caused by diffuse scattering can be clearly seen as can also the curved graphite scattering body in the foreground.
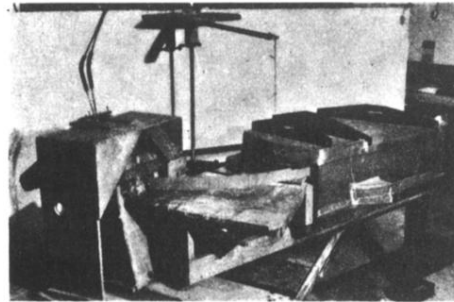
FIG. 22. General view of experimental set-up. Note the radius arm and plumb-line for locating the focal spot of the tube and the position of the scatterer. This plumb-line is aligned with the focal spot by sighting with auxiliary plumb-lines through the aperture in the tube housing at the left and through the x-ray port. The scattering angle is determined accurately by measuring the angle through which this arm rotates in passing from the focal spot to the point α_1 (Fig. 16), the angle of rotation being measured on the disk clearly visible in this figure.
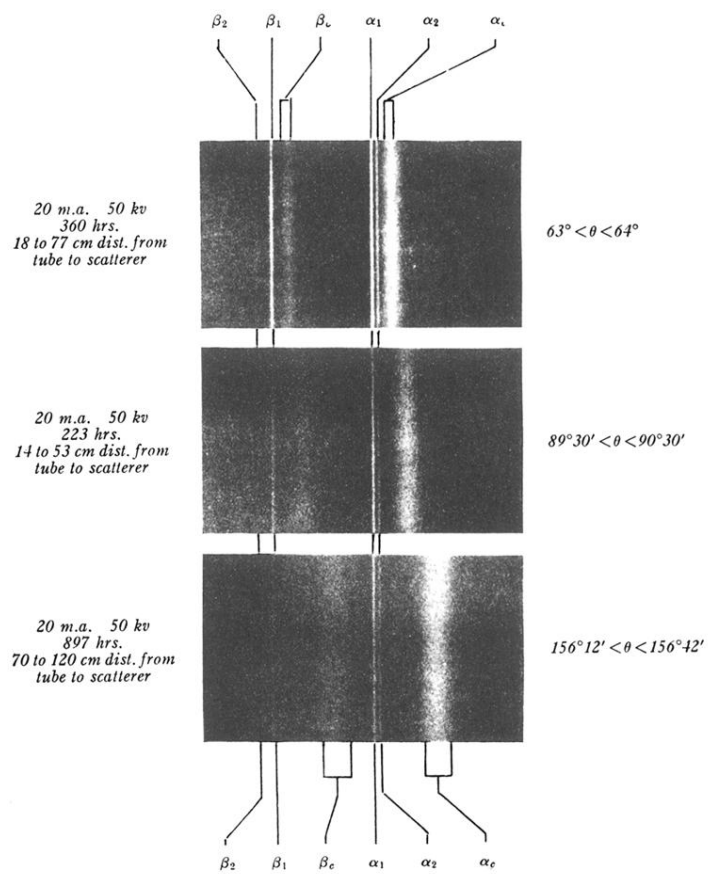
FIG. 23. Spectra of Mo K radiation scattered at three very homogeneous scattering angles from graphite, taken with the multicrystal spectrograph. Note sharpness of unshifted lines and increasing breadth of shifted lines as scattering angle increases.
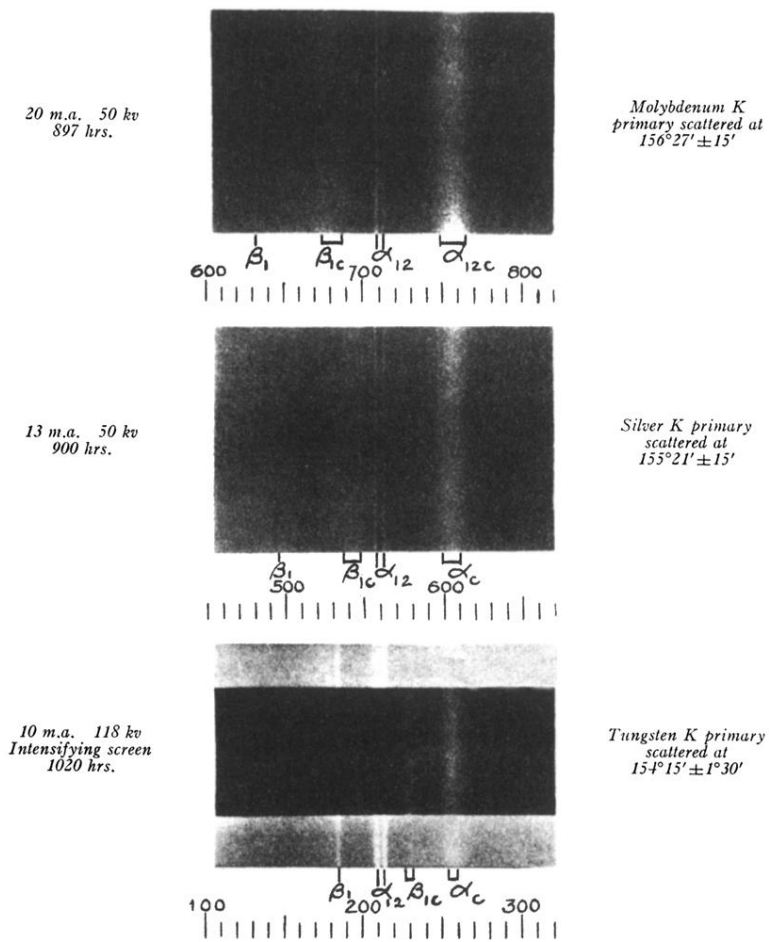
20 m.a. 50 kv
897 hrs.

*Molybdenum K
primary scattered at
156°27'±15'*

13 m.a. 50 kv
900 hrs.

*Silver K primary
scattered at
155°21'±15'*

10 m.a. 118 kv
Intensifying screen
1020 hrs.

*Tungsten K primary
scattered at
154°15'±1°30'*

FIG. 26. Three spectra of *K* radiation scattered by graphite at about 156°. The dispersion in wave-length units is the same on all three exposures as can be seen by observing that the Compton shift for the *K*α lines is the same in all three cases. (At such a large scattering angle the slight variation in scattering angle between the three cases produces no detectable difference in shift.) Note the very evident diminution in the breadth of the shifted line measured in wave-length units as the wave-length diminishes. The unshifted lines are completely absent in the case of tungsten radiation scattered from graphite. The reference lines on the edges of this film made by an auxiliary exposure with direct tungsten radiation are slightly broadened by over-exposure in combination with the effect of an intensifying screen. This is the only film on which an intensifying screen was used.